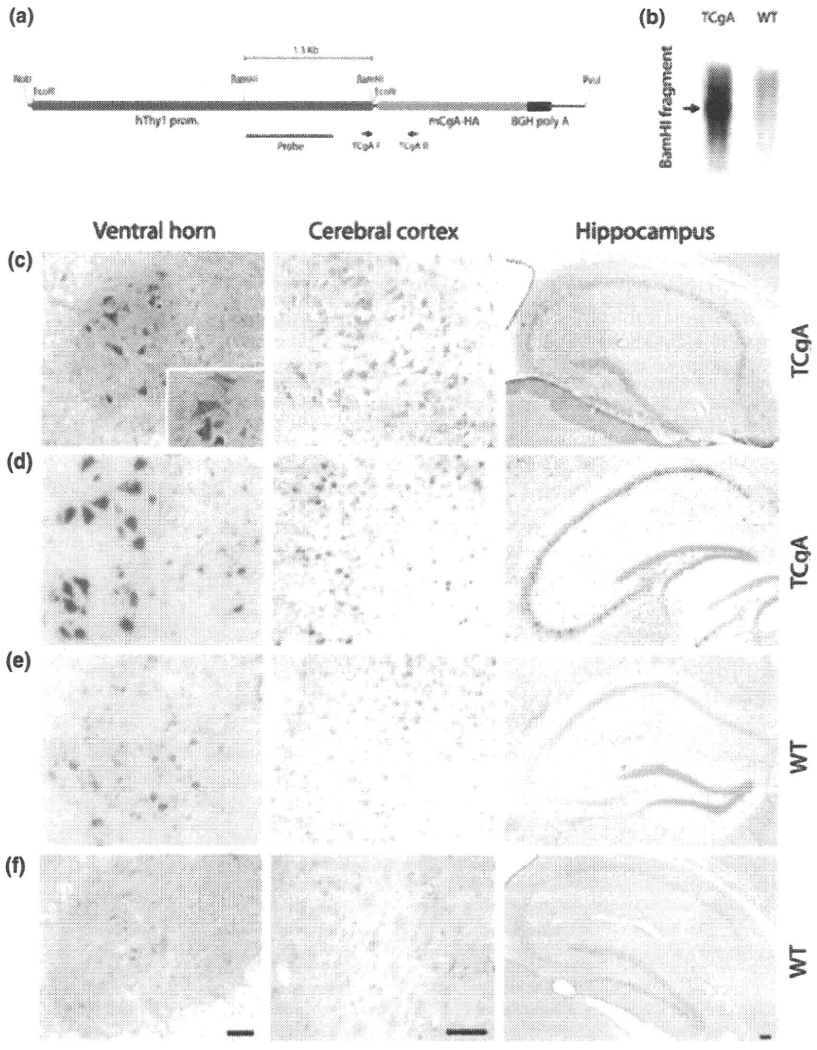

Fig. 1 Transgenic mice over-expressing CgA in neurons. (a) Partial restriction map of TCgA construct including the human Thy1 gene regulatory sequences followed by the complete coding sequence of the mouse CgA gene fused to HA. The bovine growth hormone polyadenylation (BGH-PolyA) signal is a specialized termination sequence for protein expression in eukaryotic cells. The probe used for Southern blot analysis is indicated. (b) Southern blot analysis of genomic DNA extracted from the tails of control mice (WT) and of mice bearing the TCgA transgene. (c, f) Over-expression of CgA-HA protein in different CNS tissues of TCgA mice compared to WT mice, as shown by immunohistochemistry using anti-HA monoclonal antibody. (d, e) *In situ* hybridization with CgA antisense probe showing over-expression of CgA transgene. Scale bars: 100 μm.

using HA antibody (Fig. 1c–f). In order to obtain double transgenic mice for both CgA and SOD1^{G37R}, we selected the TCgA mouse line which over-expressed the highest level of CgA in lumber motor neurons as assessed by immunohistochemistry. CgA gene expression was increased four- to fivefold in the gray matter of the lumbar spinal cord compared to non-transgenic mice, as assessed using threshold for intensity measurement of CgA mRNA signal obtained by *in situ* hybridization (Figure S1). Note that TCgA mice developed and reproduced normally transmitting the transgene in the expected Mendelian ratios.

Because there is evidence that CgA can induce an activated phenotype in microglial cells that leads to neuronal apoptosis (Ciesielski-Treska *et al.* 1998; Kingham *et al.* 1999), we analyzed microglial activation in TCgA mice by immunohistochemistry using Iba1 and Mac-2 antibodies at different ages (3, 6 and 12 months). No sign of microglial activation was detected in transgenic mice compared to normal mice (data not shown).

Neuronal over-expression of CgA in SOD1^{G37R} mice causes acceleration of disease onset

Double transgenic mice over-expressing CgA and mutant hSOD1^{G37R} (TCgA;SOD1^{G37R}) were generated by breeding mice hemizygous for TCgA and SOD1^{G37R} transgenes. Disease course was monitored by a temporal profile of the body weight and hindlimb reflex score in TCgA;SOD1^{G37R} mice. The disease onset, as defined by the time when mice reached peak body weight, occurred at mean age of 280 ± 7 days in TCgA;SOD1^{G37R} mice and at 307 ± 6 days in SOD1^{G37R} control littermates ($p < 0.05$) (Fig. 2a and b). The first signs of tremor and impairment of hindlimb extension reflex appeared in TCgA;SOD1^{G37R} mice around 4 weeks earlier than SOD1^{G37R} mice (Fig. 2c). However, the life span of ALS mice was not influenced by neuronal up-regulation of CgA (Fig. 2d; Table S2).

To further assess the effect of neuronal up-regulation of CgA on the severity of motor neuron disease induced by mutant SOD1 toxicity, quantitative pathological analysis was

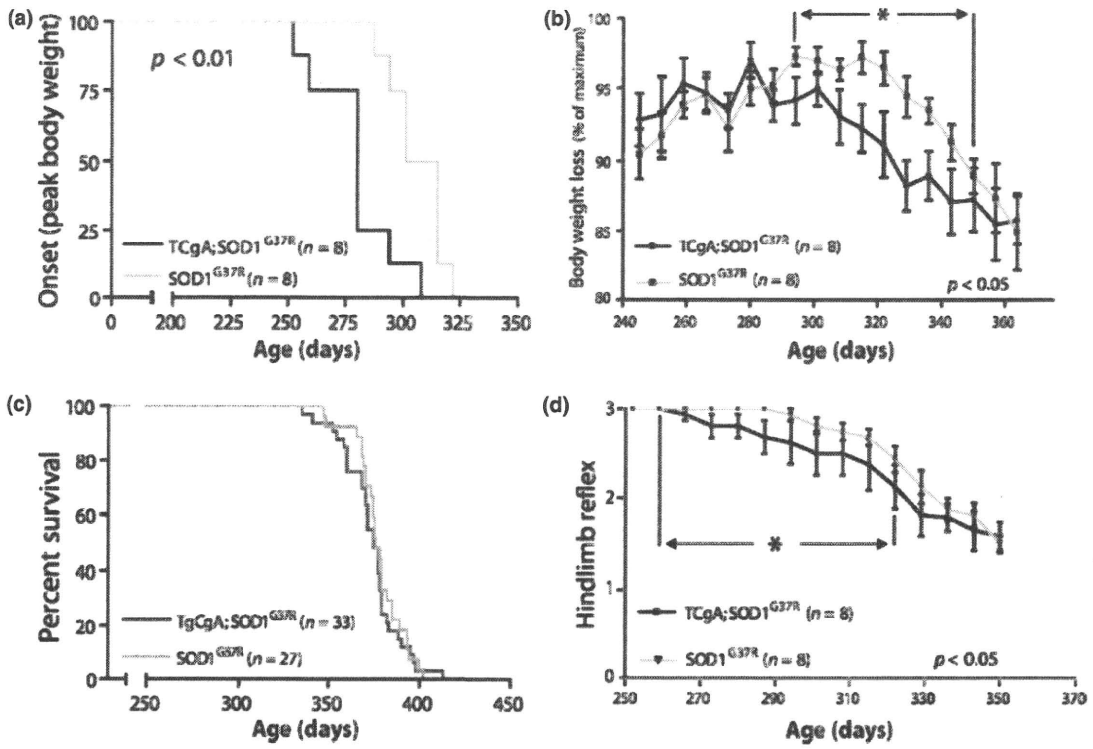

Fig. 2 Acceleration of disease onset in TCgA;SOD1^{G37R} mice. (a) Neuronal over-expression of CgA accelerated disease onset in TCgA;SOD1^{G37R} (280 ± 7 days) compared to SOD1^{G37R} (307 ± 6 days) (*$p < 0.01$, by Logrank test). (b) Disease onset was determined by the initial loss of body weight (age of peak body weight). The difference was significant for the marked time period. (c) Neuronal CgA up-regulation did not influence mortality of SOD1^{G37R} mice as shown by a Kaplan–Meier curve of survival. Double transgenic and SOD1^{G37R} mice had comparable median lifespan of 374 and 376 days, respectively. (d) The first signs of tremor and impairment of hindlimb extension reflex appeared earlier in TCgA; SOD1^{G37R} mice. Difference is significant for the marked time period. Each point indicates the average ± SEM. The data were analyzed by unpaired *t*-test.

performed at the levels of neuromuscular junctions, L5 ventral roots and spinal cord. We performed this analysis at pre-symptomatic (180 days), onset (300 days) and symptomatic stage of disease (330 days). Quantification of motor axons and lumbar spinal motor neurons at both onset and pre-symptomatic stages did not reveal differences between the two cohorts of TCgA;SOD1^{G37R} and SOD1^{G37R} mice (Figure S1b and c).

At the level of neuromuscular junction, the TCgA; SOD1^{G37R} mice exhibited a significantly higher rate of denervation at symptomatic stage, as shown by a ~ 10% decrease in intermediate end-plates and a ~ 10% increase in denervated end-plates ($p < 0.01$) (Fig. 3a). Furthermore, quantification of motor axon loss in L5 ventral roots at symptomatic stage revealed a ~ 20% increase in axonal loss in TCgA;SOD1^{G37R} mice compared to SOD1^{G37R} littermates ($p < 0.05$) (Fig. 3b and c). The TCgA;SOD1^{G37R} mice at symptomatic stage showed around 25% increase in motor neuron degeneration when compared to age control SOD1^{G37R} littermates (Fig. 4a and b).

To investigate whether acceleration of motor neuron loss was accompanied by an enhanced neuroinflammatory response, spinal cord sections were immunostained with rat anti-Mac-2 monoclonal antibody to assess microglial activation and rabbit polyclonal anti-GFAP antibody to analyse astrogliosis. Enhanced microgliosis and astrogliosis were detected in TCgA;SOD1^{G37R} mice at symptomatic stage compared to SOD1^{G37R} mice (Fig. 4c and d). Quantification of Mac-2-immunoreactive cells in sections of lumbar spinal cord displayed a higher number in double transgenic mice for both CgA and SOD1^{G37R} compared to mice hemizygote for SOD1^{G37R} ($p < 0.01$, by unpaired *t*-test) (Fig. 4e). In addition, quantification of GFAP fluorescence intensity in the lumbar spinal cord revealed a higher level of GFAP in TCgA;SOD1^{G37R} mice (Fig. 4f).

Increased levels of misfolded SOD1 species in TCgA;SOD1^{G37R} mice

Mouse monoclonal antibodies against the *apo* form of human SOD1^{G93A} mutant were generated in our laboratory (Urushitani *et al.* 2007; Gros-Louis *et al.* 2010). Interestingly, some of these antibodies (B8H10, D3H5 and A5C3) yielded distinct reactivity patterns and a high degree of specificity for a variety of mutant SOD1 species. These three monoclonals

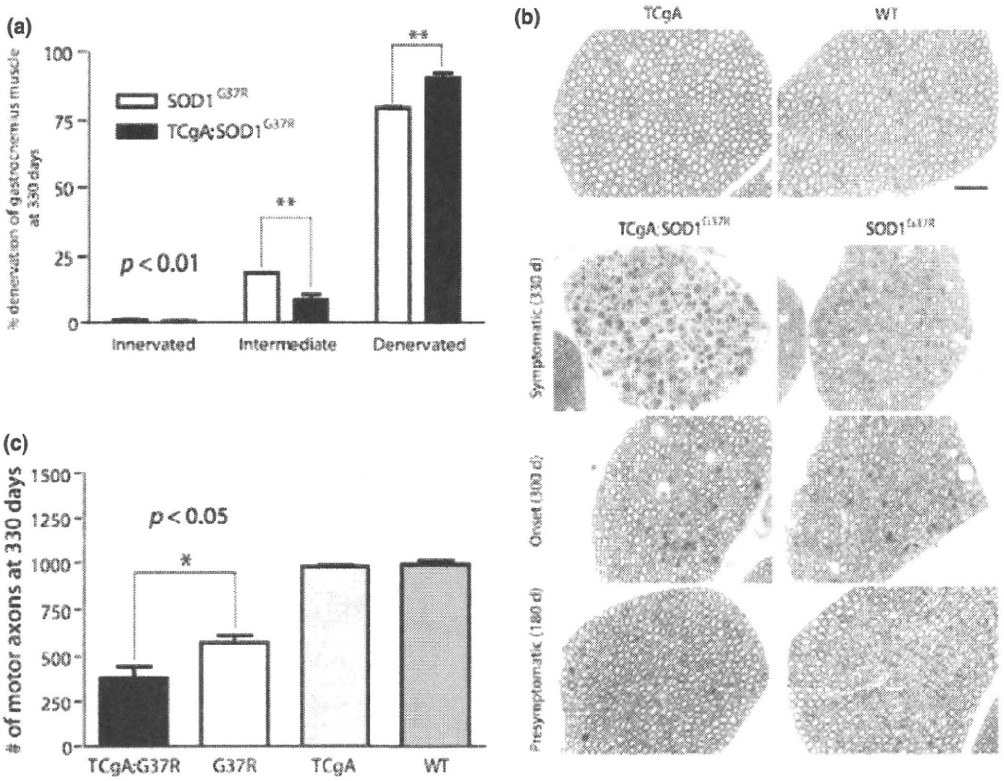

Fig. 3 Enhanced end-plate denervation and motor axon degeneration in TCgA;SOD1^{G37R} mice. (a) The co-localization of α-bungarotoxin with SV2/Synaptophysin/NF-M markers was used to evaluate the percentage of innervated, intermediate and denervated end-plates. A significant loss of innervation has been detected in gastrocnemius muscle of TCgA;SOD1^{G37R} mice at 330 days of age ($n = 3$) compared to control SOD1^{G37R} mice ($n = 3$) (**$p < 0.01$, by two-way ANOVA). (b) Toluidine blue staining of thin sections of L5 ventral root axons from pre-symptomatic, onset and symptomatic littermates of TCgA; SOD1^{G37R} and SOD1^{G37R} mice compared to TCgA and WT mice. (c) Quantitative analysis of motor axons in L5 ventral roots revealed a significant decrease (20%) in TCgA;SOD1^{G37R} ($n = 4$) as compared to SOD1^{G37R} mice ($n = 3$) at 330 days of age. (*$p < 0.01$, by unpaired *t*-test). Scale bar: 50 μm.

did not immunoprecipitate intact WT SOD1 unless it is misfolded by chelators (Gros-Louis *et al.* 2010). For instance, B8H10 antibody recognizes SOD1^{G93A} mutant and to a lower extent other mutant SOD1 forms including SOD1^{G37R} but it does not detect WT SOD1 by immunoprecipitation assay (Fig. 5a). In this study, we used B8H10 monoclonal antibody to immunoprecipitate misfolded SOD1 species from spinal cord lysates of end-stage TCgA;-SOD1^{G37R} and SOD1^{G37R} mice. Double transgenic mice yielded higher amount of immunoprecipitated SOD1 species compared to their SOD1^{G37R} littermates ($p < 0.05$) (Fig. 5b and c). Misfolded SOD1 species were detected selectively in the nervous tissue of TCgA;SOD1^{G37R} and SOD1^{G37R} mice but not in their non-neuronal tissues such as liver where the expression of CgA is normal (Fig. 5d) and where there is high level expression of mutant SOD1^{G37R} (Figure S2). Note that there was no significant change in the total amount of mutant SOD1 in the spinal cord as a result of CgA over-expression (Fig. 5e). This suggests that excess of CgA have contributed to enhance the levels of toxic misfolded forms of SOD1^{G37R}, perhaps through stabilization of these protein species.

Discussion

To elucidate the contribution of chromogranins to neurodegenerative processes of ALS caused by mutant SOD1, we generated and analyzed mice over-expressing SOD1^{G37R} in the context of CgA neuronal over-expression. Here, we report that neuronal over-expression of CgA accelerated disease onset in SOD1^{G37R} mice. Double transgenic mice for both SOD1^{G37R} and CgA developed the disease ~ 4 weeks earlier than SOD1^{G37R} littermates. Moreover, neuronal up-regulation of CgA resulted in acceleration of motor neuron degeneration in TCgA;SOD1^{G37R} mice when compared to SOD1^{G37R} control mice. The increase of motor neuron dysfunction was significant at the levels of neuromuscular junctions, L5 ventral roots and spinal cord at 330 days of age.

While the total amount of mutant SOD1 remained unchanged, immunoprecipitation analysis of spinal cord

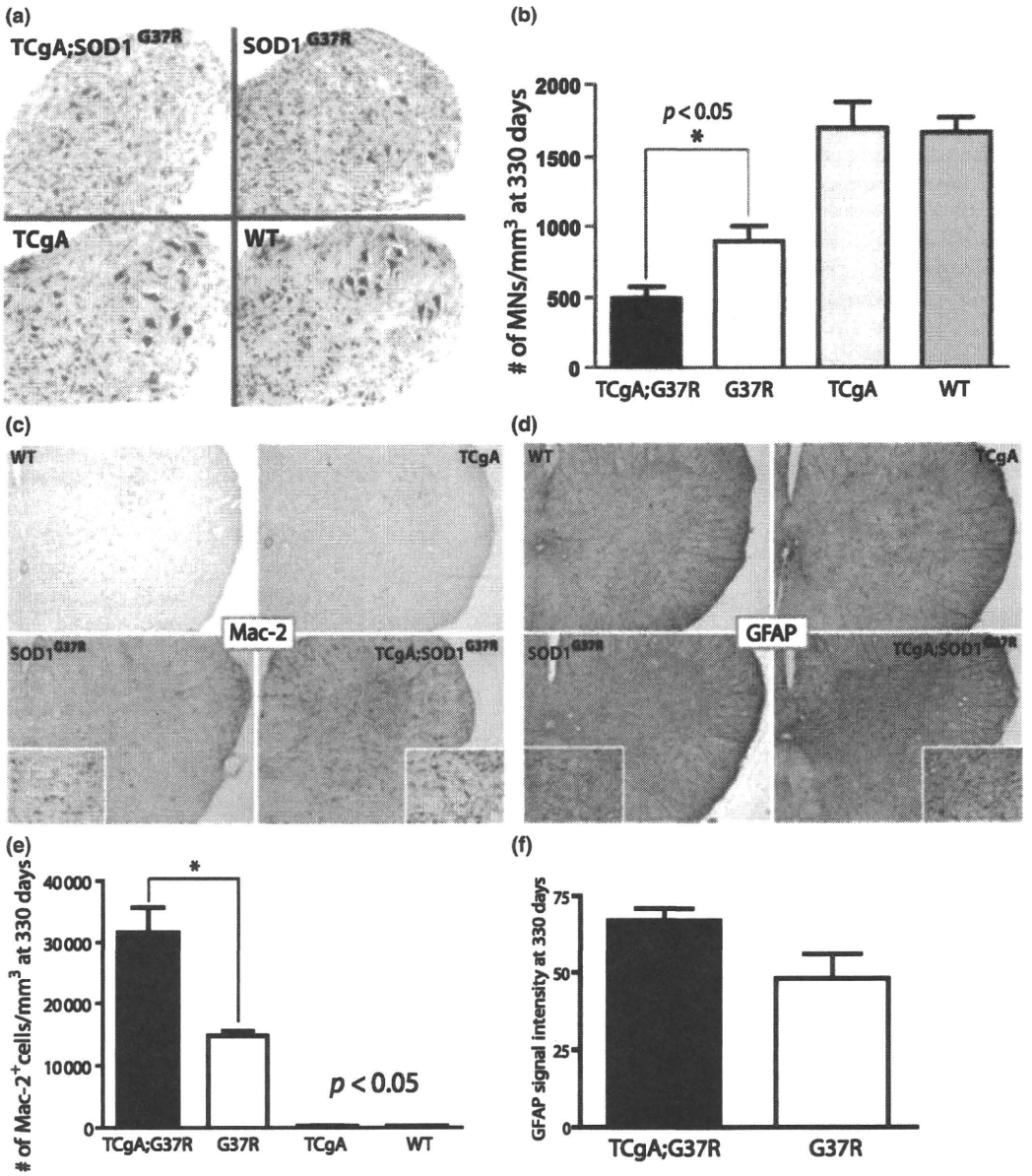

Fig. 4 Increased motor neuron loss and enhanced gliosis in TCgA;SOD1^{G37R} mice. (a) Lumbar spinal cord sections were stained with thionine following standard Nissl protocol. (b) Motor neurons were counted at different ages in TCgA;SOD1^{G37R} and SOD1^{G37R} cohorts. A significant decrease (~ 25%) in the number of motor neurons, as compared to SOD1^{G37R} mice, was detected in double transgenic mice at 330 days ($p < 0.05$, by unpaired *t*-test). (c) Immunohistochemistry of the lumbar spinal cord from symptomatic TCgA;SOD1^{G37R} and SOD1^{G37R} mice using anti-Mac-2 antibody. Note the increase in microglial cell number and Mac-2 staining in reactive microglia. (d) GFAP immunohistochemical staining of lumbar spinal cord from TCgA;SOD1^{G37R} and SOD1^{G37R} mice revealed higher immunoreactivity in double transgenic mice. (e) Significant difference in the number of Mac-2 positive cells was found between double transgenic and SOD1^{G37R} mice (*$p < 0.05$, by unpaired *t*-test). (f) In order to evaluate the astroglial reactivity, we performed immunofluorescent staining for GFAP and measured the average intensity of signal. TCgA;SOD1^{G37R} mice exhibited higher but not significant intensity of GFAP in lumbar spinal cord ($p = 0.16$ by unpaired *t*-test).

lysates using B8H10 antibody revealed enhanced levels of misfolded SOD1 species selectively in the spinal cord of TCgA;SOD1^{G37R} mice. This could explain why neuronal over-expression of CgA precipitated disease onset. Previous studies showed that the levels of mutant SOD1 expression within motor neurons is a key determinant of disease onset (Boillee *et al.* 2006). Misfolded SOD1 was not detected in non-neuronal tissues such as liver (Fig. 5d) and muscle (data not shown). The acceleration of disease onset was not accompanied by an increase in SOD1 aggregation as

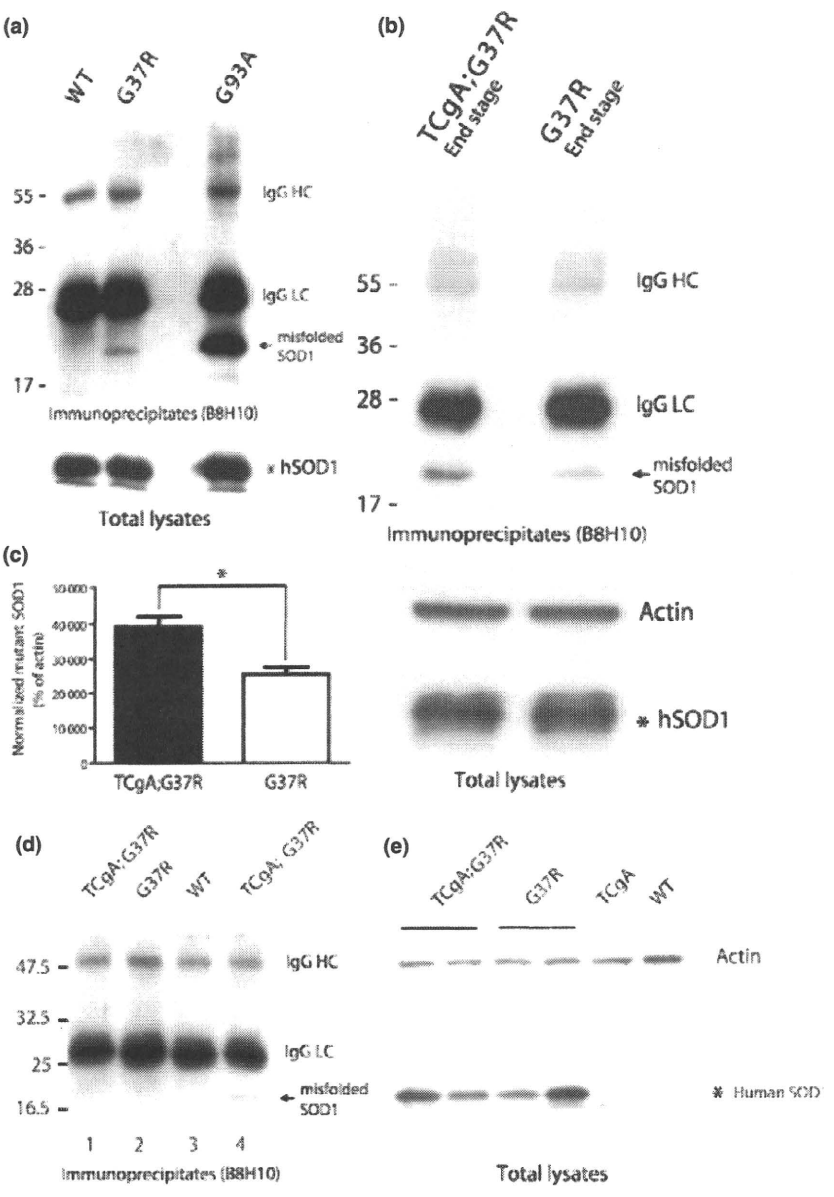

Fig. 5 Over-expression of CgA may stabilize SOD1 misfolded species. (a) Immunoprecipitation analysis of spinal cord extracts showing that the B8H10 mouse monoclonal antibody recognizes the mutant forms of SOD1 (G37R and G93A) but not the WT SOD1. Lysates were immunoprecipitated using B8H10 antibody and eluates were blotted with SOD100 antibody. (b) Immunoprecipitates with B8H10 monoclonal antibody from spinal cord extracts showing a higher amount of misfolded SOD1 species detected with SOD100 polyclonal antibody in double transgenic mice compared to SOD1^{G37R} littermates at end stage. (c) Densitometric analysis of misfolded SOD1 labelled with SOD100 antibody using actin-normalization ($p < 0.05$ by unpaired *t*-test; $n = 3$ for each group). Arrows indicate misfolded SOD1 species and asterisks indicate human SOD1. (d) Immunoprecipitates with B8H10 monoclonal antibody showing the absence of misfolded SOD1 species in non-neuronal tissues (liver at age of onset, lanes 1–3) compared to TCgA;SOD1^{G37R} neuronal tissue (spinal cord at age of onset, lane 4) as detected using SOD100 polyclonal antibody. (e) 20 μg of spinal cord protein lysates from TCgA;SOD1^{G37R} and SOD1^{G37R} mice, at age of disease onset, were subjected to SDS–PAGE. The total amount of mutant SOD1 was detected at similar levels with SOD100 antibody in TCgA;SOD1^{G37R} mice and in SOD1^{G37R} mice. * marks electrophoretic mobility of human SOD1. Densitometric analysis using actin-normalization revealed no change in total amount of mutant SOD1 in TCgA;-SOD1^{G37R} mice when compared to SOD1^{G37R} mice (data not shown).

assessed by subcellular fractionation of spinal cord lysates (data not shown).

Even though CgA over-expression in neurons precipitated disease onset, it is noteworthy that it did not affect survival. It is well established that measures of motor dysfunction and survival are separable in mice expressing mutant SOD1. For example, aspirin was able to delay onset of deficits in muscle strength of mutant SOD1 without affecting survival (Barneoud and Curet 1999), whereas riluzole prolonged survival without effects on disease onset (Gurney *et al.* 1996). Recent studies revealed that glial cells are major determinant of disease progression (Beers *et al.* 2006; Boillee *et al.* 2006; Yamanaka *et al.* 2008). Here, after disease onset, the extended symptomatic phase of TCgA;SOD1^{G37R} mice was associated with enhanced microgliosis in the spinal cord (Fig. 4c–f). It is possible that the enhanced activation of microglia in TCgA;SOD1^{G37R} mice was neuroprotective resulting in an extension of disease duration after earlier initial onset. This could explain why survival remained unchanged in TCgA;SOD1^{G37R} mice.

The effect of CgA over-expression on disease onset in ALS mice is consistent with the recent finding that ALS patients carrying a CgB gene variant (P413L variation) have an earlier age of onset as compared to those without the variation (Gros-Louis *et al.* 2009). There is evidence that the P413L variant causes retention of CgB in Golgi network with ensuing dysfunction of the secretory pathway (Gros-Louis *et al.* 2009). Moreover, we reported that chromogranins can specifically interact with SOD1 mutants to mediate secretion. Figure S1(d) shows co-localization of misfolded SOD1 with CgA-HA in

spinal motor neurons of TCgA;SOD1^{G37R} mice in vesicle-like structures. Yet, the proportion of mutant SOD1 that may be secreted via chromogranins is relatively small and hard to detect by tissue subcellular fractionation or by measuring the amount of secreted SOD1 in the cerebrospinal fluid.

Our findings that the CgB variant P413L acts as modulator of disease onset in human ALS (Gros-Louis *et al.* 2009) and that CgA over-expression precipitates disease in SOD1^{G37R} mice demonstrate key functions of chromogranins in ALS pathogenesis. Future studies are needed to determine the exact mechanisms by which chromogranins may contribute to ALS pathogenesis. Two research avenues might be promising namely the interaction of chromogranins with misfolded SOD1 species and the dysfunctions of the secretory pathway induced by excess chromogranin or CgB P413L variant. Understanding how chromogranins contribute to ALS pathogenesis could result in the development of new therapeutic approaches.

Acknowledgements

This work was supported by research grants from the ALS Society of Canada and the ALS Association (USA). We gratefully thank Geneviève Soucy, Christine Bareil, Renée Paradis, Marie-Claude Richer, Mélanie Simard, Nadia Fortin and Nicolas Audet for their assistance. We also thank Geneviève Gowing for suggestions on experiments and François Gros-Louis for his help in preparing Figure S2. Jean-Pierre Julien holds a Canada Research Chair (Tier 1) in Neurodegeneration. Makoto Urushitani holds a research grant from Japan Society of Promotion of Science (JSPS) and a Japan Health and Labour Science research grant. Samer Abou Ezzi holds a doctoral research scholarship from Fonds de la Recherche en Santé du Québec (FRSQ). The authors have no conflict of interest to declare.

Supporting information

Additional Supporting information may be found in the online version of this article:

Figure S1. (a) Dark field images of hybridized slides were recorded under identical microscope lighting and camera settings. (b) There was no significant difference in motor axonal count in L5 ventral roots at 300 days of age ($n = 4$). (c) The number of remaining motor neurons was similar between TCgA;SOD1^{G37R} and SOD1^{G37R} mice ($n = 4$). (d) Immunofluorescence using anti-HA and B8H10 antibodies shows co-localization of misfolded SOD1 and CgA-HA in spinal motor neurons of TCgA;SOD1^{G37R} mice. Arrows mark the sites of colocalization.

Figure S2. Detection of human SOD1^{G37R} protein by immunoblotting after SDS–PAGE of total proteins from spinal cord and liver of transgenic SOD1^{G37R} mice and of non-transgenic mice.

Table S1. Primers used for genotyping of transgenic.

Table S2. Average and median lifespan of TCgA;SOD1^{G37R}.

As a service to our authors and readers, this journal provides supporting information supplied by the authors. Such materials are peer-reviewed and may be re-organized for online delivery, but are not copy-edited or typeset. Technical support issues arising from supporting information (other than missing files) should be addressed to the authors.

References

Barneoud P. and Curet O. (1999) Beneficial effects of lysine acetylsalicylate, a soluble salt of aspirin, on motor performance in a transgenic model of amyotrophic lateral sclerosis. *Exp. Neurol.* **155**, 243–251.

Beaulieu J. M., Nguyen M. D. and Julien J. P. (1999) Late onset of motor neurons in mice overexpressing wild-type peripherin. *J. Cell Biol.* **147**, 531–544.

Beers D. R., Henkel J. S., Xiao Q., Zhao W., Wang J., Yen A. A., Siklos L., McKercher S. R. and Appel S. H. (2006) Wild-type microglia extend survival in PU.1 knockout mice with familial amyotrophic lateral sclerosis. *Proc. Natl Acad. Sci. USA* **103**, 16021–16026.

Boillee S., Yamanaka K., Lobsiger C. S., Copeland N. G., Jenkins N. A., Kassiotis G., Kollias G. and Cleveland D. W. (2006) Onset and progression in inherited ALS determined by motor neurons and microglia. *Science* **312**, 1389–1392.

Ciesielski-Treska J., Ulrich G., Taupenot L., Chasserot-Golaz S., Corti A., Aunis D. and Bader M. F. (1998) Chromogranin A induces a neurotoxic phenotype in brain microglial cells. *J. Biol. Chem.* **273**, 14339–14346.

Couse J. F., Davis V. L., Tally W. C. and Korach K. S. (1994) An improved method of genomic DNA extraction for screening transgenic mice. *BioTechniques* **17**, 1030–1032.

Fiesel F. C., Voigt A., Weber S. S. *et al.* (2010) Knockdown of transactive response DNA-binding protein (TDP-43) downregulates histone deacetylase 6. *EMBO J.* **29**, 209–221.

Gowing G., Philips T., Van Wijmeersch B., Audet J. N., Dewil M., Van Den Bosch L., Billiau A. D., Robberecht W. and Julien J. P. (2008) Ablation of proliferating microglia does not affect motor neuron degeneration in amyotrophic lateral sclerosis caused by mutant superoxide dismutase. *J. Neurosci.* **28**, 10234–10244.

Gros-Louis F., Andersen P. M., Dupre N. *et al.* (2009) Chromogranin B P413L variant as risk factor and modifier of disease onset for amyotrophic lateral sclerosis. *Proc. Natl Acad. Sci. USA* **106**, 21777–21782.

Gros-Louis F., Soucy G., Lariviere R. and Julien J. P. (2010) Intracerebroventricular infusion of monoclonal antibody or its derived Fab fragment against misfolded forms of SOD1 mutant delays mortality in a mouse model of ALS. *J. Neurochem.* **113**, 1188–1199.

Gurney M. E. (1994) Transgenic-mouse model of amyotrophic lateral sclerosis. *N. Engl. J. Med.* **331**, 1721–1722.

Gurney M. E., Cutting F. B., Zhai P., Doble A., Taylor C. P., Andrus P. K. and Hall E. D. (1996) Benefit of vitamin E, riluzole, and gabapentin in a transgenic model of familial amyotrophic lateral sclerosis. *Ann. Neurol.* **39**, 147–157.

Helle K. B. (2004) The granin family of uniquely acidic proteins of the diffuse neuroendocrine system: comparative and functional aspects. *Biol. Rev. Camb. Philos. Soc.* **79**, 769–794.

Kingham P. J., Cuzner M. L. and Pocock J. M. (1999) Apoptotic pathways mobilized in microglia and neurones as a consequence of chromogranin A-induced microglial activation. *J. Neurochem.* **73**, 538–547.

Laflamme N., Lacroix S. and Rivest S. (1999) An essential role of interleukin-1beta in mediating NF-kappaB activity and COX-2 transcription in cells of the blood-brain barrier in response to a systemic and localized inflammation but not during endotoxemia. *J. Neurosci.* **19**, 10923–10930.

Lobsiger C. S., Boillee S., McAlonis-Downes M., Khan A. M., Feltri M. L., Yamanaka K. and Cleveland D. W. (2009) Schwann cells expressing dismutase active mutant SOD1 unexpectedly slow disease progression in ALS mice. *Proc. Natl Acad. Sci. USA* **106**, 4465–4470.

Marksteiner J., Lechner T., Kaufmann W. A., Gurka P., Humpel C., Nowakowski C., Maier H. and Jellinger K. A. (2000) Distribution of chromogranin B-like immunoreactivity in the human hippocampus and its changes in Alzheimer's disease. *Acta Neuropathol.* **100**, 205–212.

Nguyen M. D., Lariviere R. C. and Julien J. P. (2001) Deregulation of Cdk5 in a mouse model of ALS: toxicity alleviated by perikaryal neurofilament inclusions. *Neuron* **30**, 135–147.

Nishimura M., Tomimoto H., Suenaga T., Nakamura S., Namba Y., Ikeda K., Akiguchi I. and Kimura J. (1994) Synaptophysin and chromogranin A immunoreactivities of Lewy bodies in Parkinson's disease brains. *Brain Res.* **634**, 339–344.

Rangon C. M., Haik S., Faucheux B. A., Metz-Boutigue M. H., Fierville F., Fuchs J. P., Hauw J. J. and Aunis D. (2003) Different chromogranin immunoreactivity between prion and a-beta amyloid plaque. *Neuroreport* **14**, 755–758.

Rosen D. R., Siddique T., Patterson D. *et al.* (1993) Mutations in Cu/Zn superoxide dismutase gene are associated with familial amyotrophic lateral sclerosis. *Nature* **362**, 59–62.

Schiffer D., Cordera S., Giordana M. T., Attanasio A. and Pezzulo T. (1995) Synaptic vesicle proteins, synaptophysin and chromogranin A in amyotrophic lateral sclerosis. *J. Neurol. Sci.* **129**(Suppl), 68–74.

Schrott-Fischer A., Bitsche M., Humpel C., Walcher C., Maier H., Jellinger K., Rabl W., Glueckert R. and Marksteiner J. (2009) Chromogranin peptides in amyotrophic lateral sclerosis. *Regul. Pept.* **152**, 13–21.

Taupenot L., Harper K. L. and O'Connor D. T. (2003) The chromogranin-secretogranin family. *N. Engl. J. Med.* **348**, 1134–1149.

Urushitani M., Sik A., Sakurai T., Nukina N., Takahashi R. and Julien J. P. (2006) Chromogranin-mediated secretion of mutant superoxide dismutase proteins linked to amyotrophic lateral sclerosis. *Nat. Neurosci.* **9**, 108–118.

Urushitani M., Ezzi S. A. and Julien J. P. (2007) Therapeutic effects of immunization with mutant superoxide dismutase in mice models of amyotrophic lateral sclerosis. *Proc. Natl Acad. Sci. USA* **104**, 2495–2500.

Urushitani M., Ezzi S. A., Matsuo A., Tooyama I. and Julien J. P. (2008) The endoplasmic reticulum-Golgi pathway is a target for translocation and aggregation of mutant superoxide dismutase linked to ALS. *FASEB J.* **22**, 2476–2487.

Yamanaka K., Chun S. J., Boillee S., Fujimori-Tonou N., Yamashita H., Gutmann D. H., Takahashi R., Misawa H. and Cleveland D. W. (2008) Astrocytes as determinants of disease progression in inherited amyotrophic lateral sclerosis. *Nat. Neurosci.* **11**, 251–253.

Zhao W., Beers D. R., Henkel J. S., Zhang W., Urushitani M., Julien J. P. and Appel S. H. (2009) Extracellular mutant SOD1 induces microglial-mediated motoneuron injury. *Glia* **58**, 231–243.

免疫療法によるALSの分子標的治療

Molecular targetting by immunotherapy in ALS

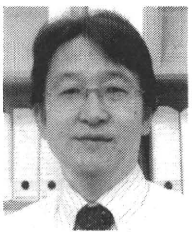

漆谷　真
Makoto URUSHITANI
滋賀医科大学分子神経科学研究センター神経難病治療学分野

◎筋萎縮性側索硬化症(ALS)は全身の骨格筋の進行性萎縮と機能低下を主体とする神経変性疾患である．1993年にスーパーオキシドジスムターゼ1(SOD1)の突然変異が家族性ALSの20%に存在することが判明し，変異SOD1トランスジェニック(Tg)マウスがALSと類似の病態を示したことから，ALSのモデル動物として病態解析が精力的になされた．その結果，運動ニューロンのみに変異SOD1が発現しても神経変性は起こらず，周囲に変異SOD1を発現するグリア細胞が取り囲むことが必要であるという非細胞自律性運動ニューロン死の概念が確立した．著者らはその機序を研究するなかで，変異SOD1が神経分泌蛋白であるクロモグラニンと結合し，細胞外に分泌されることでミクログリアを活性化し，運動ニューロン死を傷害することを見出した．さらに，細胞外SOD1を標的としたワクチン療法と抗血清由来の抗SOD1抗体の脳室内投与によって変異SOD1Tgマウスの進行を抑制することに成功した．一方，著者らは数種類の変異SOD1特異認識モノクローナル抗体の開発に成功し，そのひとつがALSモデルマウスの他動免疫に有効であることが最近報告された．さらに近年，種々の神経変性疾患において病原蛋白の細胞外分泌や伝播性と疾患の進行との関連が注目されており，抗体による分子標的治療は有効な治療選択肢として期待されている．

Key word：筋萎縮性側索硬化症(ALS)，トランスジェニックマウス，ワクチン，抗体療法，細胞外分泌仮説

筋萎縮性側索硬化症(amyotrophic lateral sclerosis：ALS)は全身の骨格筋の進行性萎縮と機能低下を主体とする神経変性疾患である．病理学的には，大脳皮質運動野から脳幹や脊髄へ至る一次運動ニューロン(皮質脊髄路，皮質橋路，皮質延髄路)と，二次運動ニューロン(運動性脳神経と前角細胞)の選択的な変性を主徴とする系統変性の形をとる．1869年にフランスの神経内科医，Jean-Martin Charcot(シャルコー)らが2名のALS症例の臨床病理所見を報告[1]してから140年以上経過したが，以来1990年初頭まで大きな学術的進歩はなく，われわれ神経内科医のALSに関する知識はシャルコーのそれとほとんど変わるところはなかった．

ところが，1993年に家族性ALSの20%でスーパーオキシドジスムターゼ1(superoxide dismutase 1：SOD1)の突然変異が発見され[2]，さらに変異SOD1トランスジェニック(Tg)マウス(「サイドメモ1」参照)が優れたALSモデルマウスとし

サイドメモ1　トランスジェニックマウス

遺伝子工学的技術を用いて，マウスの受精卵にヒトの病原遺伝子などの外来遺伝子を導入し，目的の遺伝子を強制的に発現させたマウス．疾患関連候補遺伝子の導入により罹患者と同様の表現型や病理所見を示した場合，当該遺伝子の疾患関連性の証明となり，疾患モデルマウスとして治療研究上重要である．変異SOD1トランスジェニックマウスはヒトALS関連遺伝子を有する初のALSモデルマウスである．

て世に出現して以来[3]，ALSにおける情報量は飛躍的に増加した．本稿ではこうした流れのなかで発見された変異SOD1蛋白のユニークな物性と，変異SOD1 Tgマウスに対する免疫療法研究について紹介する．さらに近年では，TAR DNA-binding protein-43(TDP-43)やfused in sarcoma(FUS)などあらたな病因遺伝子が明らかとなっており，分子標的治療法としての免疫療法が有するSOD1以外のALS治療への潜在性についても述べてみたい．

変異SOD1を有する家族性ALS

ALSの10%が明らかな家族歴を有し，さらにその20%のALS患者でSOD1に突然変異が認められる．SOD1はスーパーオキシドを過酸化水素と酸素に分解する抗酸化酵素であり，活性中心に銅(Cu)と亜鉛(Zn)が配位結合し，二量体(ダイマー)を形成している．153アミノ酸からなる比較的低分子の蛋白質であるが，現在まで120種類以上のアミノ酸残基で突然変異体が報告され，その酵素活性がさまざまであることから，変異による効果は抗酸化作用の機能低下(loss of function)ではなく，異常蛋白質としてのあらたな有害機能の獲得(gain of toxic function)であると考えられている．すべてのSOD1変異体に共通する，野生型SOD1と異なる化学物性は，翻訳後正常な折りたたみ(フォールディング)を受けずに正常構造を逸脱した状態(ミスフォールド状態)をとることである．その結果，疎水性が高くなり，オリゴマーや凝集体を形成しやすくなる．また，細胞内ではheat shock protein 70などの熱ショックシャペロンと結合し，またユビキチン-プロテアソーム経路(「サイドメモ2」参照)で分解される．

変異SOD1が細胞内で過剰に発現した場合，さまざまな異常現象が誘発され，細胞死に至る．たとえば，野生型SOD1はおもに細胞質に存在する一方，ミトコンドリアや小胞体への異所性局在や蓄積が起こる．また，プロテアソーム経路分解能の低下や，軸索輸送の障害が起こることが報告されている．このように当該細胞内の異常現象によって生じる細胞死を細胞自律性死という．

サイドメモ2　ユビキチン-プロテアソーム経路

転写・翻訳後に正常に折りたたまれなかった蛋白質や，変異型の蛋白質は，ユビキチンポリユビキチン鎖が付加された後，プロテアソームに移動し，数種類のプロテアーゼによって分解される．この過程はユビキチン活性化酵素(E1)，ユビキチン変換酵素(E2)，ユビキチンリガーゼ(E3)のおもに三者によってATP依存性に進行される．多くの神経変性疾患でユビキチン陽性の封入体が認められることから，プロテアソーム分解系と神経変性との関連が疑われている．

免疫療法の根拠となるALSの病態

1. 非細胞自律性運動ニューロン死

その一方，変異SOD1 Tgマウスの解析が進むにつれて興味深い事実が判明してきた．それは，変異SOD1による運動ニューロン死は運動ニューロン内の変異SOD1のみでは不十分であり，周囲を取り巻くアストログリアやミクログリアなどの細胞で変異SOD1が発現していることが必要という，運動ニューロン死の非細胞自律性である．驚くべきことに，たとえ運動ニューロンに変異SOD1が発現していなくとも，周囲を変異SOD1発現細胞に取り囲まれるとその運動ニューロンは死滅する[4]．さらに近年，ALS以外のAlzheimer病，Parkinson病，Huntington病といった神経変性疾患の神経細胞死も非細胞自律性のある可能性が指摘されている[5]．非細胞自律性ニューロン死の理解は治療戦略上非常に重要である．たとえば，運動ニューロンの移植治療を行っても周囲のグリア細胞によってふたたび変性が起こる可能性がある．

2. 変異SOD1分泌仮説とプリオノイド仮説

非細胞自律性運動ニューロン死の背景には，運動ニューロンとグリア細胞を結ぶ何らかのシグナル物質の存在が考えられる．これまでにNagaiらが変異SOD1を発現するアストロサイトから低分子の運動ニューロン障害物質が分泌されることを報告し，Di Giorgioらはそれがプロスタグランジン D2であると報告している[5]．

一方著者らは，ミスフォールドした変異SOD1蛋白質自体が神経分泌蛋白質であるクロモグラニ

ン(「サイドメモ3」参照)と結合して細胞外に分泌され，ミクログリアの活性化や運動ニューロン死を起こすことを示した．つまり疾患の原因蛋白質自体が細胞外で“danger molecule”として非細胞自律性ニューロン死を起こしうることを示しており[7]，近年，このSOD1のみならず，タウ蛋白質，シヌクレイン，Huntingtinといった病原蛋白質が細胞内でβシート構造や何らかのミスフォールド構造をとるとプリオン蛋白質のように播種性になりうるという“プリオノイド(prionoid)”仮説が提唱されている[8,9]．

たいへん興味深いことに，Parkinson病[10]，Huntington病[11]患者に対する細胞移植治療で移植細胞は正常に生着したが，シヌクレインやHuntingtin蛋白質が移植細胞内で，蓄積していたことが報告されており，ミスフォールド蛋白質病理が伝播する現象が本仮説と何らかの関連性を有している可能性もある．ALSにおいても最近，変異SOD1 Tgマウスの脊髄病巣においてミスフォールドSOD1がアミロイドフィブリル様構造体をつくり周囲に拡大していることが報告されている[12]．細胞質蛋白質が細胞外に分泌される機序は不明であるが，小胞体-Golgi体を介しない非古典的経路や，exoxomeを介した細胞間の受け渡しなどが提唱されている．このプリオノイド仮説は神経変性疾患における病巣拡大の機序のひとつとしてたいへん注目されている．

サイドメモ3　クロモグラニン(chromogranin)

下垂体や副腎皮質などの神経分泌組織やその他の内分泌組織で分泌される酸性蛋白質で，保存配列からクロモグラニンAとBが存在する．カテコールアミンなどの分泌物質とともに放出されると同時に，とくにクロモグラニンAはその切断断片がストレスや血圧，炎症反応に関連することが報告されている．著者らは，クロモグラニンA，Bが変異SOD1と結合し，分泌を促進すること，細胞外の変異SOD1がミクログリアを活性化し，運動ニューロン死をきたすことを報告した[7]．さらに近年，クロモグラニンBのある遺伝子多型がカナダ，スウェーデン，フランスの孤発性・家族性ALS患者の危険因子であり，発症促進因子であることが報告された[23]

3. 獲得免疫系とALSの病態

ALSの病巣においてCD4，CD8⁻Tリンパ球が集積することは古くから報告されていたが[13]，中枢神経系は末梢循環から免疫学的に隔絶されていることから(免疫特権；immune previlege)，その一義的役割は不明であった．しかし近年，ALS患者の脳脊髄液のみならず，末梢血においても腫瘍壊死因子(TNF)，インターロイキン1β(IL-1β)，インターフェロンγ(IFN-γ)などの炎症性サイトカインが上昇していることが報告された[14,15]．T細胞とALSの病態との関連は変異SOD1 Tgマウスを用いた研究でつぎつぎと解明されている．

Beersらは，CD4ノックアウトマウスと変異SOD1Tgマウスを交配させ，CD4陽性Tリンパ球が運動ニューロン変性を抑制していることを報告した[16]．一方，Chiuらは変異SOD1 TgマウスのT細胞抗原受容体β鎖(TCRβ)を欠失させるとALS症状が増悪することを示した．彼らの報告によれば，TCRβノックアウトマウスの脊髄病巣においてミクログリアのインスリン様成長因子(IGF-Ⅰ)の発現が低下しており，このIGF-ⅠはT細胞から分泌されるインターロイキン4(IL-4)が誘導する．その一方でIFN-γは，ミクログリアの表面抗原をMCHⅡにシフトさせ，細胞性免疫系を誘導する[17]．

以上の知見は，末梢循環系のT細胞と中枢のミクログリアとのクロストークと中枢神経系におけるTh1/Th2などの獲得免疫系のバランスがALSの病態に密接にかかわる可能性を示している．

細胞外SOD1を標的とした免疫療法

著者らは上述の経過から，細胞外の変異SOD1蛋白質を標的として変異SOD1 Tgマウスに対するワクチン療法を行った．まず，37番目のグリシンがアルギニンに置換され，内因性SOD1の5倍程度変異蛋白質が発現しているG37R型SOD1 Tgマウス(低発現型Tgマウス)に対して異なる変異型であるG93A型の組換え変異SOD1蛋白質をワクチンとして接種したところ，発症時期を遅延させ，進行も有意に抑制した(図1-A)．ところが，変異SOD1の発現量が内因性17倍と高く，

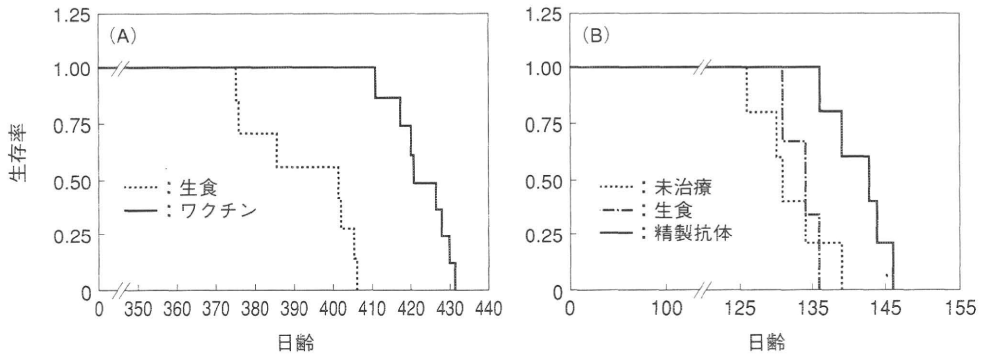

図 1　変異SOD1トランスジェニックマウスに対する免疫療法の効果

A：変異蛋白質の発現量が低い低発現型(G37R 型)SOD1 Tg マウスに対するワクチンの効果．組換え G93A 型 SOD1 蛋白質を 60 日齢のマウスに Ribi アジュバントとともに 4 回ワクチン投与を行った．変異 SOD1 ワクチン投与群は，生理食塩水(生食)と Ribi アジュバントを投与した対照群に比べて寿命が 30 日間延長した．また，発症時期も 20 日間延長した．

B：発症時期(90 日齢)の高発現型(G93A 型)SOD1 Tg マウスに，変異 SOD1(G93A)組換え蛋白質で免疫した抗血清から精製した抗体を脳室内持続投与した．その結果，抗体投与群は生理食塩水対照群や未治療群に比べ 7 日間進行を遅延させた．

G37R 型に比べ早期に発症し寿命も短い G93A SOD1 Tg マウス(高発現型 Tg マウス)では同じワクチンが無効であった．一方，正常マウスに変異 SOD1 ワクチンを投与して得られた抗血清由来の抗体を，発症前後の高発現 Tg マウスの脳室内に持続投与したところ，寿命を有意に延長した(図 1-B)[18]．また著者らは，アポ状態の野生型 SOD1 がミスフォールド状態を以前に報告していたが[19]，アポ型野生型 SOD1 によるワクチン療法の有効性も確認している[20]．

ワクチンは投与回数が少なく非侵襲的であることから今後，野生型 SOD1 をベースとしたワクチンは特定の遺伝子変異によらない有効な治療法として有望である．しかし，Alzheimer 病に対する抗アミロイドワクチンの臨床治験において一定の割合で脳炎が生じたように，ワクチンには同時に獲得免疫系を介した副作用が生じる可能性も高い．そこで IL-4 などの抗炎症性サイトカインが誘導される Th2 系が優位となるようにアジュバントやワクチンの投与経路，さらに抗原部位の設定を工夫することが必要となる．

一方，ワクチンによる副作用を排除して免疫療法を行うためには，病原蛋白を標的とした特異抗体の利用が有用である．著者らは変異型 SOD1 を特異的に認識するマウスモノクローナル抗体を数種類つくることに成功した[18]．Gros-Louis らはそのなかの 1 種類(D3H5 クローン)を発症前後の高発現 G93A SOD1 Tg マウスの脳室内に持続注入し，抗血清とほぼ同様の進行抑制効果を認めた[21]．興味深いことに，D3H5 抗体は貪食細胞との結合に関与する定常部の一部である Fc 領域を除いた可変部領域(Fab)のみでも，ある程度の進行抑制効果を認めている．その機序は不明であるが，細胞外変異 SOD1 の病原性の高い特定の配列を中和している可能性がある．近年，細胞 SOD1 においてミクログリアの活性化にかかわるアミノ酸配列が同定されており[22]，本抗体の作用機序との関連においてたいへん興味深い．著者らは，D3H5 とは異なるモノクローナル抗体の脊髄髄腔内持続投与がさらに有効であることを確認しており，その作用機序について現在解析中である(未報告)．

分子標的療法としての免疫療法

変異 SOD1 の分泌仮説にとどまらず現在，Alzheimer 病，Parkinson 病，Huntington 病においてもプリオノイド仮説に基づく病原蛋白の細胞外・細胞間作用が注目されており，細胞外の病原蛋白を攻撃対象とした免疫療法は治療薬として大きな可能性を有する．さらに，抗体に特定のシグナルペプチド(HIV の TAT 配列など)を付加することに

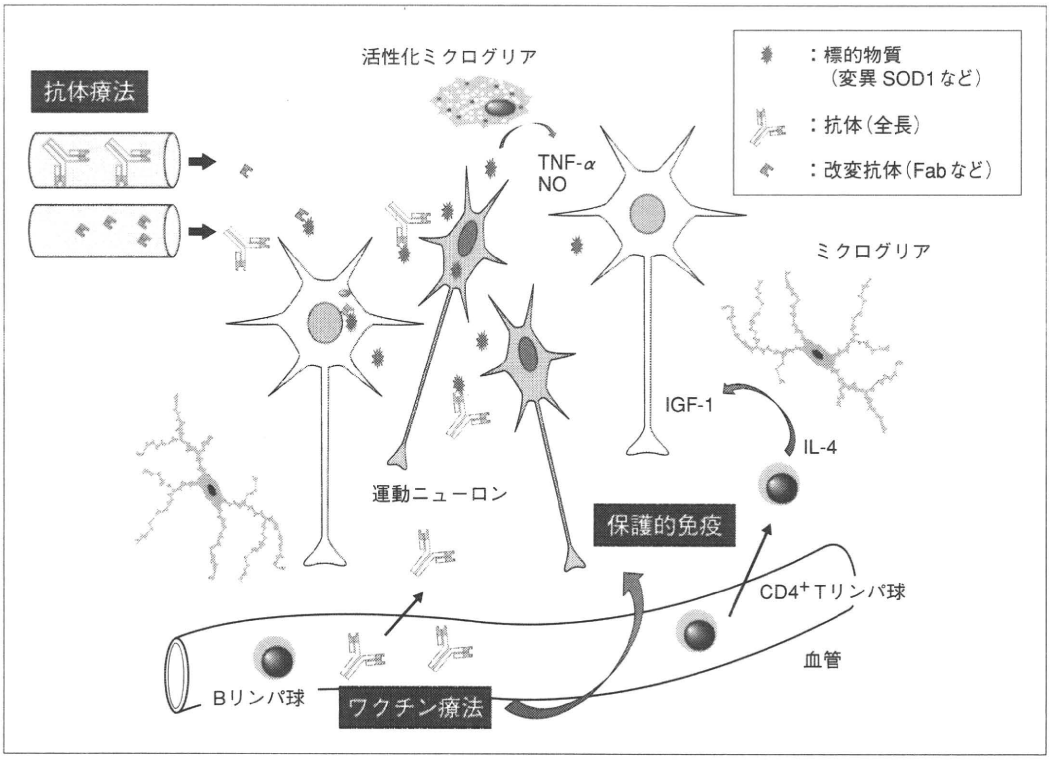

図 2　ALSに対する免疫療法のストラテジー

ミスフォールドした変異 SOD1 は細胞内で多彩な毒性を及ぼすと同時に細胞外に分泌され，ミクログリアの活性化や周囲の細胞へ毒性を伝播すると考えられている．ワクチン療法は細胞外の原因物質の除去を主眼とするが，同時に動員される獲得免疫反応が保護的シグナルになるように治療戦略の工夫が必要である．原因蛋白質に対する特異抗体の直接投与（他動免疫）も細胞外因子の除去に有効と考えられるが，可変領域の Fab 抗体を応用した抗体の改良によって細胞内の標的分子に対するアクセスも可能となる．青矢印は神経保護的因子，赤矢印は神経毒性に関与する因子．

よって，抗体の細胞内への移行性を高めることが可能である．

近年の抗体の開発技術の進歩はめざましく，マウスで得られたモノクローナル抗体のヒト化や，可変領域からなる一本鎖抗体（single chain variable fragment：ScFV）を，抗体ファージライブラリー技術や，ハイブリドーマの cDNA を用いて高効率に合成する技術などが確立している．そして抗体療法の適応は標的分子の除去にとどまらず，病原分子における特定のアミノ酸構造を標的とした病原蛋白質の活性・機能調節作用も論理的には可能であり，抗体療法は神経変性疾患の治療の選択肢として有望である．今後は神経変性疾患の標的抗原を効果的に同定する方法の開発が望まれる．

おわりに

以上，ALS における免疫療法の現状と今後の展望について概説した．現時点では変異 SOD1 Tg マウスにおいて治療効果が確認されたところであり，今後，家族性 ALS 患者に対する臨床応用に向けた研究が展開されている．また，孤発性 ALS においても今後 T，DP-43 Tg マウスなどあらたなモデル動物の解析によって治療標的構造が明らかになれば，新規免疫療法の開発研究が進むものと期待される．

文献

1) Charcot, J. M. et al.：*Archives de Physiologie Normale et Pathologique*, **2**：354-367, 1869.
2) Rosen, D. R. et al.：*Nature*, **362**：59-62, 1993.
3) Gurney, M. E. et al.：*Science*, **264**：1772-1775, 1994.

4) Clement, A. M. et al. : *Science*, **302** : 113-117, 2003.
5) Ilieva, H. et al. : *J. Cell Biol.*, **187** : 761-772, 2009.
6) Di Giorgio, F. P. et al. : *Cell Stem Cell*, **3** : 637-648, 2008.
7) Urushitani, M. et al. : *Nat. Neurosci.*, **9** : 108-118, 2006.
8) Aguzzi, A. et al. : *Neuron*, **64** : 783-790, 2009.
9) Frost, B. et al. : *Nat. Rev. Neurosci.*, **11** : 155-159, 2010.
10) Li, J. Y. et al. : *Nat. Med.*, **14** : 501-503, 2008.
11) Cicchetti, F. et al. : *Proc. Natl. Acad. Sci. USA*, **106** : 12483-12488, 2009.
12) Chia, R. et al. : *PLoS One*, **5** : e10627, 2010.
13) Kawamata, T. et al. : *Am. J. Pathol.*, **140** : 691-707, 1992.
14) Tateishi, T. et al. : *J. Neuroimmunol.*, **222** : 76-81, 2010.
15) Babu, G. N. et al. : *Neurochem. Res.*, **33** : 1145-1149, 2008.
16) Beers, D. R. et al. : *Proc. Natl. Acad. Sci. USA*, **105** : 15558-15563, 2008.
17) Chiu, I. M. et al. : *Proc. Natl. Acad. Sci. USA*, **105** : 17913-17918, 2008.
18) Urushitani, M. et al. : *Proc. Natl. Acad. Sci. USA*, **104** : 2495-2500, 2007.
19) Urushitani, M. et al. : *J. Neurochem.*, **90** : 231-244, 2004.
20) Takeuchi, S. et al. : *J. Neuropathol. Exp. Neurol.*, 2010(Epub ahead of print).
21) Gros-Louis, F. et al. : *J. Neurochem.*, **113** : 1188-1199, 2010.
22) Hernandez, S. et al. : *J. Neuropathol. Exp. Neurol.*, **69** : 176-187, 2010.
23) Gros-Louis, F. et al. : *Proc. Natl. Acad. Sci. USA*, **106** : 21777-21782, 2009.

*　　*　　*

THE JOURNAL OF BIOLOGICAL CHEMISTRY VOL. 285, NO. 45, pp. 34885–34898, November 5, 2010

Seeded Aggregation and Toxicity of α-Synuclein and Tau

CELLULAR MODELS OF NEURODEGENERATIVE DISEASES[*S]

Received for publication, May 26, 2010, and in revised form, August 17, 2010 Published, JBC Papers in Press, August 30, 2010, DOI 10.1074/jbc.M110.148460

Takashi Nonaka[‡1], **Sayuri T. Watanabe**[‡§], **Takeshi Iwatsubo**[§¶], **and Masato Hasegawa**[‡2]

From the [‡]*Department of Molecular Neurobiology, Tokyo Institute of Psychiatry, Tokyo 156-8585 and the* [§]*Department of Neuropathology and Neuroscience, Graduate School of Pharmaceutical Science, and* [¶]*Department of Neuropathology, Graduate School of Medicine, University of Tokyo, Tokyo 113-0033, Japan*

The deposition of amyloid-like filaments in the brain is the central event in the pathogenesis of neurodegenerative diseases. Here we report cellular models of intracytoplasmic inclusions of α-synuclein, generated by introducing nucleation seeds into SH-SY5Y cells with a transfection reagent. Upon introduction of preformed seeds into cells overexpressing α-synuclein, abundant, highly filamentous α-synuclein-positive inclusions, which are extensively phosphorylated and ubiquitinated and partially thioflavin-positive, were formed within the cells. SH-SY5Y cells that formed such inclusions underwent cell death, which was blocked by small molecular compounds that inhibit β-sheet formation. Similar seed-dependent aggregation was observed in cells expressing four-repeat Tau by introducing four-repeat Tau fibrils but not three-repeat Tau fibrils or α-synuclein fibrils. No aggregate formation was observed in cells overexpressing three-repeat Tau upon treatment with four-repeat Tau fibrils. Our cellular models thus provide evidence of nucleation-dependent and protein-specific polymerization of intracellular amyloid-like proteins in cultured cells.

The conversion of certain soluble peptides and proteins into insoluble filaments or misfolded amyloid proteins is believed to be the central event in the etiology of a majority of neurodegenerative diseases (1–4). Alzheimer disease (AD)[3] is characterized by the deposition of two kinds of filamentous aggregates, extracellular deposits of β-amyloid plaques composed of amyloid β (Aβ) peptides, and intracellular neurofibrillary lesions consisting of hyperphosphorylated Tau. In Parkinson disease (PD) and dementia with Lewy bodies (DLB), filamentous inclusions consisting of hyperphosphorylated α-synuclein (α-syn) are accumulated in degenerating neurons (5). The deposition of prion proteins in synapses and extracellular spaces is the defining characteristic of Creutzfeldt-Jakob disease and other prion diseases (3). The identification of genetic defects associated with early onset AD, familial PD, frontotemporal dementia, parkinsonism linked to chromosome 17 (caused by Tau mutation and deposition), and familial Creutzfeldt-Jakob disease has led to the hypothesis that the production and aggregation of these proteins are central to the development of neurodegeneration. Fibrils formed of Aβ display a prototypical cross-β-structure characteristic of amyloid (6), as do many other types of filaments deposited in the extracellular space in systemic or organ-specific amyloidoses (7), including prion protein deposits (8). Filaments assembled from α-syn (9) and from Tau filaments (10) were also shown to possess cross-β-structure, as were synthetic filaments derived from exon 1 of huntingtin with 51 glutamines (11). It therefore seems appropriate to consider neurodegenerative disorders developing intracellular deposits of amyloid-like proteins as brain amyloidosis. The accumulation and propagation of extracellular amyloid proteins are believed to occur through nucleation-dependent polymerization (12, 13). However, it has been difficult to establish the relevance of this process in the *in vivo* situation because of the lack of a suitable cell culture model or method to effectively introduce seeds into cells. For example, it has not yet been possible to generate *bona fide* fibrous inclusions reminiscent of Lewy bodies as a model of PD by overexpressing α-syn in neurons of transgenic animals. Here, we describe a novel method for introducing amyloid seeds into cultured cells using lipofection, and we present experimental evidence of seed-dependent polymerization of α-syn, leading to the formation of filamentous protein deposits and cell death. This was also clearly demonstrated in cells expressing different Tau isoforms by introducing the corresponding Tau fibril seeds.

EXPERIMENTAL PROCEDURES

Chemicals and Antibodies—A phosphorylation-independent antibody Syn102 and monoclonal and polyclonal antibodies against a synthetic phosphopeptide of α-syn (Ser(P)^{129}) were used as described previously (5). Polyclonal anti-ubiquitin antibody was obtained from Dako. Polyclonal anti-Tau Ser(P)^{396} was obtained from Calbiochem. Monoclonal anti-α-tubulin and anti-HA clone HA-7 were obtained from Sigma. Lipofectamine was purchased from Invitrogen. Monoclonal

* This work was supported by grants-in-aid for scientific research on Priority Areas, Research on Pathomechanisms of Brain Disorders (to T. I. and M. H.) and Grant-in-aid for Scientific Research (C) 19590297 and 22500345 (to T. N.) from the Ministry of Education, Culture, Sports, Science, and Technology of Japan.

[S] The on-line version of this article (available at http://www.jbc.org) contains supplemental Figs. S1–S5.

[1] To whom correspondence may be addressed: Dept. of Molecular Neurobiology, Tokyo Institute of Psychiatry 2-1-8 Kamikitazawa, Setagaya-ku, Tokyo 156-8585, Japan. Tel.: 81-3-3304-5701; Fax: 81-3-3329-8035; E-mail: nonaka-tk@igakuken.or.jp.

[2] To whom correspondence may be addressed: Dept. of Molecular Neurobiology, Tokyo Institute of Psychiatry 2-1-8 Kamikitazawa, Setagaya-ku, Tokyo 156-8585, Japan. Tel.: 81-3-3304-5701; Fax: 81-3-3329-8035; E-mail: hasegawa-ms@igakuken.or.jp.

[3] The abbreviations used are: AD, Alzheimer disease; Aβ, amyloid β; PD, Parkinson disease; DLB, dementia with Lewy bodies; α-syn, α-synuclein; 3R1N, three-repeat Tau isoform with one amino-terminal insert; 4R1N, four-repeat Tau isoform with one amino-terminal insert; LA, Lipofectamine; LDH, lactate dehydrogenase.

anti-Tau T46 was from Zymed Laboratories Inc.. AT100 and HT7 antibodies were obtained from Innogenetics.

Preparation of α-Syn Seed, Oligomers, and Tau Fibrils—Human α-syn cDNA in bacterial expression plasmid pRK172 was used to produce recombinant protein (14). Wild-type (WT) or carboxyl-terminally HA-tagged α-syn was expressed in *Escherichia coli* BL21 (DE3) and purified as described (15). To obtain α-syn fibrils, α-syn (5–10 mg/ml) was incubated at 37 °C for 4 days with continuous shaking. The samples were diluted with 5 volumes of 30 mM Tris-HCl buffer (pH 7.5) and ultracentrifuged at 110,000 × *g* for 20 min at 25 °C. The pellets were resuspended in 30 mM Tris-HCl buffer (pH 7.5) and sonicated twice for 5 s each. The protein concentration was determined as described, and this preparation was used as Seed αS. In the case of α-syn oligomers, α-syn (10 mg/ml) was incubated at 37 °C for 3 days in the presence of 10 mM exifone. After incubation, the mixture was ultracentrifuged at 110,000 × *g* for 20 min at 25 °C. The supernatant was desalted by Sephadex G-25 (Amersham Biosciences) column chromatography, and eluted fractions (α-syn oligomers) were analyzed by reversed-phase HPLC, SDS-PAGE, and immunoblot analysis. Recombinant human three-repeat Tau isoform with one amino-terminal insert (3R1N) and four-repeat Tau isoform with one amino-terminal insert (4R1N) monomer and corresponding fibrils were prepared as described previously (16, 17).

Introduction of Proteins into Cells—Human neuroblastoma SH-SY5Y cells obtained from ATCC were cultured in DMEM/F-12 medium with 10% FCS. Cells at ~30–50% confluence in 6-well plates were treated with 200 μl of Opti-MEM containing 2 μg of the seed α-syn WT (Seed αS); HA-tagged α-syn (Seed-HA); α-syn monomers, oligomers; or Tau 3R1N or 4R1N fibrils; and 5 μl of Lipofectamine (LA) for 3 h at 37 °C. The medium was changed to DMEM/F-12, and culture was continued for 14 h. The cells were collected by treatment with 0.5 ml of 0.25% trypsin for 10 min at 37 °C, followed by centrifugation (1,800 × *g*, 5 min) and washing with PBS. The cellular proteins were extracted with 100 μl of homogenization buffer containing 50 mM Tris-HCl, pH 7.5, 0.15 M NaCl, 5 mM EDTA, and a mixture of protease inhibitors by sonication. After ultracentrifugation at 290,000 × *g* for 20 min at 4 °C, the supernatant was collected as a Tris-soluble fraction, and the protein concentration was determined by BCA assay. The pellet was solubilized in 100 μl of SDS-sample buffer. Both Tris-soluble and insoluble fractions were analyzed by immunoblotting with appropriate antibodies as indicated (15, 18).

Cell Culture Model of Seed-dependent Polymerization of α-Syn or Tau—α-Syn or Tau 3R1N or 4R1N was transiently overexpressed in SH-SY5Y cells by transfection of 1 μg of wild-type human α-syn cDNA in pcDNA3 (pcDNA3-α-syn) or human Tau cDNA in pcDNA3 (pcDNA3-Tau 3R1N or 4R1N) with 3 μl of FuGENE6 (Roche Applied Science) in 100 μl of Opti-MEM, followed by culture for 14 h. Under our experimental conditions, the efficiency of transfection with pEGFP-C1 vector was 20–30%. The cells were washed with PBS once, and then Seed αS, Seed-HA, Seed 3R1N, or Seed 4R1N was introduced with Lipofectamine as described above. The medium was changed to DMEM/F-12, and culture was continued for ~2–3 days. Cells were harvested in the presence of trypsin to digest extracellular cell-associated α-syn fibrils. The cellular proteins were differentially extracted and immunoblotted with the indicated antibodies, as described (18).

Confocal Microscopy—SH-SY5Y cells on coverslips were transfected with pcDNA3-α-syn and cultured for 14 h as described above, and then Seed αS was introduced, and culture was continued for ~1–2 days. After fixation with 4% paraformaldehyde, the cells were stained with appropriate primary and secondary antibodies as described previously (18). For thioflavin S staining, the cells were incubated with 0.05% thioflavin S at room temperature for 5 min. Fluorescence was analyzed with a laser-scanning confocal fluorescence microscope (LSM5Pascal, Carl Zeiss).

Immunoelectron Microscopy—For electron microscopy, cells overexpressing α-syn were transfected with Seed αS, cultured for 2 days, fixed in 0.1 M phosphate buffer containing 4% glutaraldehyde for 12 h, and then processed and embedded in LR White resin (London Resin, Reading, UK). Ultrathin sections were stained with uranyl acetate for investigation. Immunolabeling of the inclusions was performed by means of an immunogold-based postembedding procedure. Sections were blocked with 10% calf serum, incubated overnight on grids with anti-Ser(P)^{129} antibody at a dilution of 1:100, rinsed, then reacted with secondary antibody conjugated to 10-nm gold particles (E-Y Laboratories, San Mateo, CA) (1:10), rinsed again and stained with uranyl acetate.

Immunoelectron microscopic analysis of α-syn or Tau filaments extracted from cells was performed as follows. Cells overexpressing α-syn or Tau were transfected with Seed αS or Seed Tau, respectively. After incubation for 3 days, they were harvested, suspended in 200 μl of 10 mM Tris-HCl, pH 7.4, 1 mM EGTA, 10% sucrose, 0.8 M NaCl) and sonicated. The lysates were centrifuged at 20,400 × *g* for 20 min at 4 °C. The supernatant was recovered, and Sarkosyl was added (final 1%, v/v). The mixtures were incubated at room temperature for 30 min and then centrifuged at 113,000 × *g* for 20 min. The resulting pellets were suspended in 30 mM Tris-HCl, pH 7.5, placed on collodion-coated 300-mesh copper grids, and stained with the indicated antibodies and 2% (v/v) phosphotungstate. Micrographs were recorded on a JEOL 1200EX electron microscope.

Cell Death Assay—Cell death assay was performed using a CytoTox 96 non-radioactive cytotoxicity assay kit (Promega). TUNEL staining was performed using an *in situ* cell death detection kit (Roche Applied Science).

Assay of Proteasome Activity—SH-SY5Y cells transfected with pcDNA3-α-syn and Seed αS were cultured for 3 days or treated with 20 μM MG132 for 4 h. Cells were harvested, and cytosolic fraction was prepared as follows. Cells were resuspended in 100 μl of phosphate-buffered saline (PBS) and disrupted by sonication, and then insoluble material was removed by ultracentrifugation at 290,000 × *g* for 20 min at 4 °C. The supernatant was assayed for proteasome activity by using a fluorescent peptide substrate, benzyloxycarbonyl-Leu-Leu-Glu-7-amido-4-methylcoumarin (Peptide Institute, Inc.). 7-Amino-4-methylcoumarin release was measured fluorometrically (excitation at 365 nm; emission at 460 nm). In a green fluorescent protein (GFP) reporter assay of proteasome activity in living cells by confocal laser microscopy, SH-SY5Y cells trans-

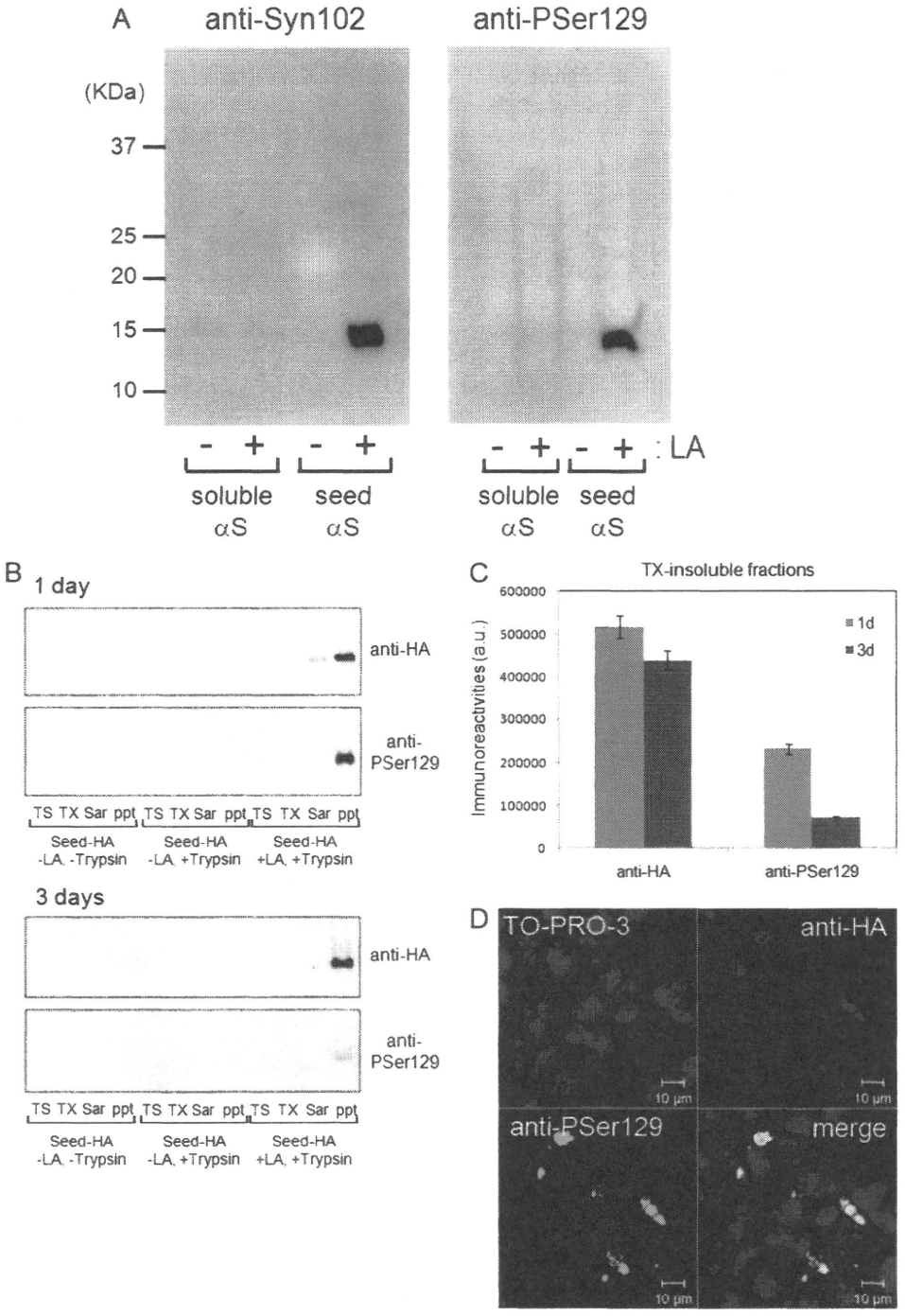

FIGURE 1. **Introduction of seed α-syn into cultured cells with Lipofectamine reagent.** *A*, purified recombinant α-syn (soluble form; 2 μg) and filaments (2 μg) were sonicated and then incubated with LA. The protein-LA complexes were dispersed in Opti-MEM and added to SH-SY5Y cells. After 14 h of culture, the cells were collected and sonicated in SDS sample buffer. After boiling, the samples were analyzed by immunoblotting with a phosphorylation-dependent anti-α-syn Ser(P)^{129} (*PSer129*) (*right*) or a phosphorylation-independent antibody, Syn102 (*left*). *B* and *C*, carboxyl-terminally HA-tagged α-syn fibril seeds (*Seed-HA*) were transduced into cells by the use of LA. After incubation for 1 day (*1d*) or 3 days (*3d*), cells were harvested with or without trypsin, and proteins were differentially extracted from the cells with Tris-HCl (*TS*), Triton X-100 (*TX*), and Sarkosyl (*Sar*), leaving the pellet (*ppt*). Immunoblot analyses of lysates using anti-HA and anti-Ser(P)^{129} are shown. The immunoreactive band positive for anti-HA or anti-Ser(P)^{129} in the Triton X-100-insoluble fraction was quantified. The results are expressed as means ± S.E. (n = 3). *D*, confocal laser microscopic analysis of cells treated with Seed-HA in the presence of LA. Cells were transduced with 2 μg of Seed-HA using 5 μl of LA. After a 48-h incubation, cells were fixed and immunostained with anti-Ser(P)^{129} (*green*) and anti-HA (*red*) and counterstained with TO-PRO-3 (*blue*).

fected with pcDNA3-α-syn (1 μg) and GFP-CL1 (0.3 μg) using FuGENE6 and then transfected with Seed αS were grown on coverslips for 2 days or treated with 20 μM MG132 for 6 h (19). These cells were analyzed using a laser-scanning confocal fluorescence microscope (LSM5Pascal, Carl Zeiss).

Statistical Analysis—The p values for the description of the statistical significance of differences were calculated by means of the unpaired, two-tailed Student's t test using GraphPad Prism 4 software (GraphPad Software).

RESULTS

Introduction of Seed α-Syn into Cultured Cells Using Lipofectamine Reagent—Cellular overexpression of α-syn by itself does not lead to fibrillization of α-syn in a form that resembles Lewy bodies. This prompted us to examine whether or not introduction of preformed aggregation seeds of α-syn (Seed αS) would elicit fibril formation. To introduce Seed αS into SH-SY5Y cells in a non-invasive manner, we tried several reagents used for transporting proteins or plasmid DNA into cells and found that LA, a cationic gene introducer, enables the introduction of Seed αS into SH-SY5Y cells. We were not able to detect any introduced α-syn monomer or fibrils following the simple addition of protein preparations to the culture medium, notwithstanding a previous report on this approach (20). The insoluble α-syn formed following LA-mediated Seed αS introduction was detected as buffer-insoluble α-syn in cell lysates (Fig. 1*A*). The insoluble α-syn was phosphorylated at Ser^{129} upon introduction into cells (Fig. 1*A*), indicating that Seed αS was incorporated in cells and phosphorylated intracellularly. Cells were harvested in the presence of trypsin to digest extracellular cell-associated α-syn fibrils. The optimal ratio of LA to Seed αS was about 5 μl to 2 μg of protein in 6-well plates. This treatment effectively introduced Seed αS not only into SH-SY5Y cells but also into several other types of cells examined, including Chinese hamster ovary cells and human embryonic kidney 293T cells (data not shown). In sharp contrast, soluble α-syn (either monomeric or oligomeric forms) was not introduced into the

cells by the same treatment (Figs. 1*A* and 4), suggesting that the LA treatment works exclusively for the internalization of insoluble α-syn aggregates.

These results strongly suggest that α-syn fibrils are incorporated with the aid of LA but do not exclude the possibility that extracellular α-syn fibrils may induce aggregation of endogenous α-syn without incorporation. To confirm that the extracellular α-syn fibril seeds are internalized into cells by LA, we performed the transduction of preformed carboxyl-terminally HA-tagged α-syn fibril seeds (Seed-HA) instead of non-tagged

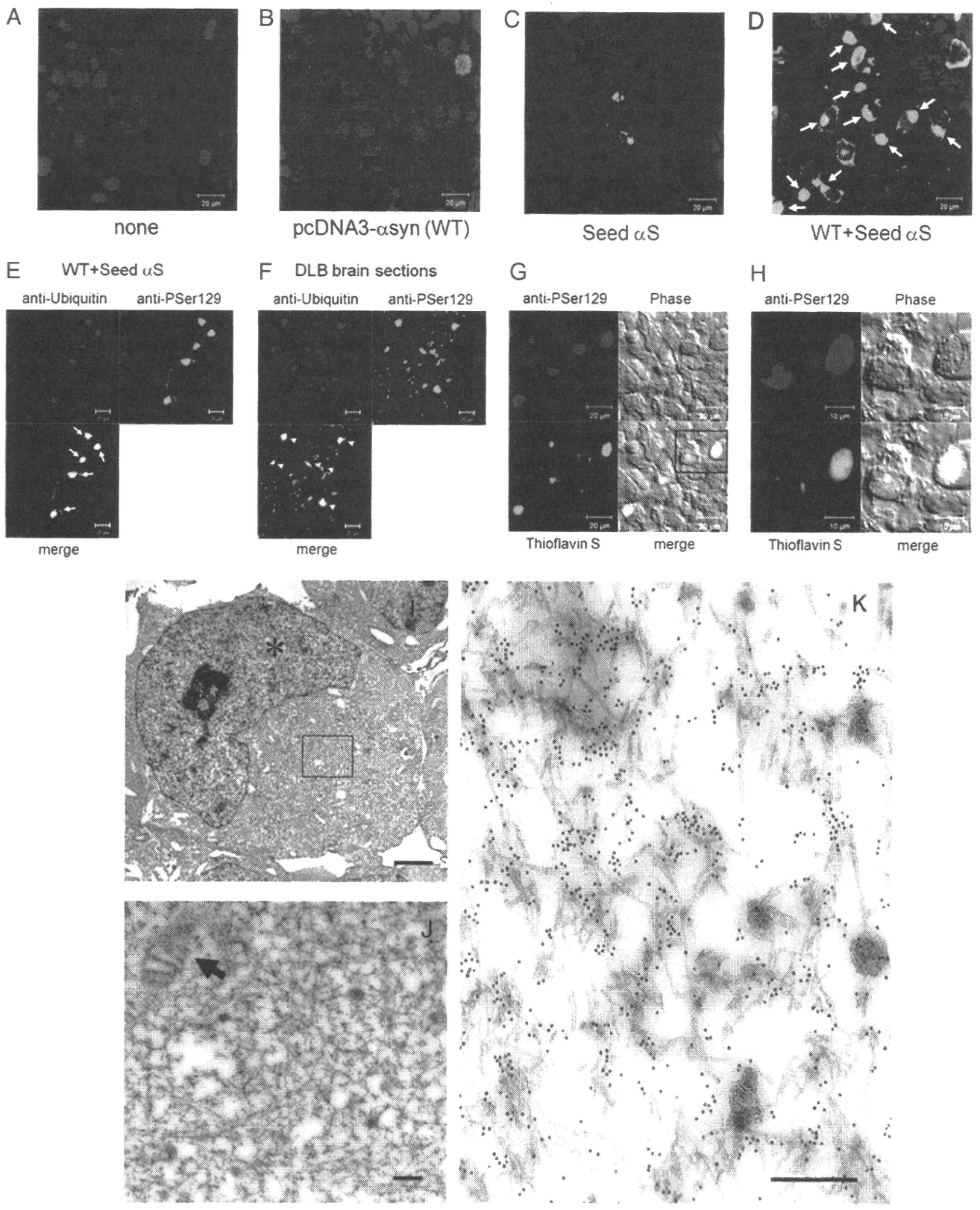

α-syn seeds. As shown in Fig. 1, *B* and *C*, time course experiments revealed that Seed-HA was also incorporated into cells in the presence of LA and could be detected with both anti-HA antibody and a phospho-α-syn-specific antibody (anti-Ser(P)^{129}), even 3 days after infection. Confocal microscopic analyses also indicated that Seed-HA was phosphorylated at Ser^{129} intracellularly. All anti-Ser(P)^{129}-positive dotlike structures were also stained with anti-HA, indicating that no endogenously phosphorylated α-syn aggregates are present in the cells (Fig. 1*D* and supplemental Fig. S1*C*).

Establishment of a Cell Culture Model for Nucleation-dependent Polymerization of α-Syn—Although introduction of the seed α-syn into cells was accompanied with phosphorylation, no further dramatic change was observed. Because the level of endogenous α-syn was relatively low in SH-SY5Y cells, we introduced non-tagged or HA-tagged seeds into cells transiently overexpressing α-syn. After 3 days of culture, immunocytochemistry for α-syn revealed a diffuse (Fig. 2*B*) or dotlike (Fig. 2*C*) pattern of cytoplasmic labeling by anti-Ser(P)^{129} in cells transfected with wild-type α-syn without seeds or in non-overexpressing cells with Seed αS, respectively. Surprisingly, however, in cells transfected with both pcDNA3-α-syn and Seed αS, we observed abundant round inclusions that occupied the cytoplasm and displaced the nucleus, with morphology highly reminiscent of cortical-type Lewy bodies observed in human brain (Fig. 2*D*). The size of the α-syn-positive inclusions was ~10 μm in diameter (Fig. 2*D*), which is similar to that of the Lewy bodies detected in the brains of patients with dementia with Lewy bodies. Similarly, when cells expressing α-syn were transfected with Seed-HA, abundant phosphorylated α-syn-positive cells were also detected (supplemental Fig. S1*D*).

We next examined the status of ubiquitin, which is positive in most types of intracellular filamentous inclusions, including Lewy bodies, in neurodegenerative disease brains. As shown in Fig. 2*E*, we found that almost all intracellular inclusions labeled with anti-Ser(P)^{129} were also positive for ubiquitin, as is the case for Lewy bodies in the cortex of human DLB brain (Fig. 2*F*). Furthermore, the juxtanuclear Ser(P)^{129}-positive, Lewy body-like inclusions were also positively labeled with thioflavin S, a fluorescent dye that specifically intercalates within structures rich in β-pleated sheet conformation (Fig. 2, *G* and *H*), indicating that the inclusions contain β-sheet-rich filamentous aggregates. Electron microscopic analysis of cells transfected with both wild-type α-syn and the seeds revealed that the inclusions are composed of filamentous structures ~10 nm in diameter that are often covered with granular materials (Fig. 2, *I* and *J*). The filamentous structures were randomly oriented within the cytoplasm of these cells, forming a meshwork-like profile, and were frequently intermingled with mitochondria (Fig. 2, *I* and *J*), being highly reminiscent of human cortical Lewy bodies. Immunoelectron microscopy showed that the filaments were densely decorated with anti-Ser(P)^{129} (Fig. 2*K*), demonstrating that they were composed of phosphorylated α-syn.

To biochemically validate this cellular model and to investigate further the molecular mechanisms underlying nucleation-dependent aggregation within cells, we differentially extracted α-syn from these cells using detergents of various strengths and analyzed the extracts by immunoblotting with anti-Syn102 and -Ser(P)^{129} antibodies. The levels of α-syn in the Sarkosyl-soluble and -insoluble fractions (total α-syn and α-syn phosphorylated at Ser^{129}, respectively) were dramatically increased in cells transfected with both wild-type α-syn and the seeds (*WT + Seed αS* in Fig. 3, *A* and *B*). To distinguish endogenous α-syn from exogenous α-syn fibrils, we used LA to transduce Seed-HA into cells overexpressing α-syn. Immunoblot analyses of these cells showed that HA-tagged α-syn with slower mobility than non-tagged α-syn was detected in the Sarkosyl-insoluble pellets as phosphorylated forms by anti-HA and anti-Ser(P)^{129} antibodies in cells treated with Seed-HA + LA (Fig. 3, *C–E*). Interestingly, in cells expressing α-syn (WT) treated with Seed-HA + LA, much more abundant non-tagged α-syn was detected in the Triton X-100- and Sarkosyl-insoluble fractions as phosphorylated forms with a smaller amount of the HA-α-syn. We also performed a dose dependence experiment with Seed-HA in cells expressing α-syn. As shown in supplemental Fig. S2, immunoreactive levels of Triton X-100-insoluble phosphorylated α-syn increased in parallel with an increase in the amount of Seed-HA. Furthermore, we tested whether Tau protein forms intracellular aggregates in the presence of α-syn seeds instead of Tau seeds. We found that Tau was not aggregated with Seed-HA, confirming that intracellular aggregate formation of soluble α-syn is specific to and dependent on fibril seeds of the same protein (supplemental Fig. S3). This nucleation-dependent polymerization of α-syn in cells was greater at 3 days than at 1 day after transduction of the seeds (Fig. 3*F*).

Negative stain electron microscopic observation of Sarkosyl-insoluble fractions of the cells harboring inclusions revealed anti-Syn102 and Ser(P)^{129}-positive filaments of ~5–10-nm width (Fig. 3, *G* and *H*) that are highly reminiscent of those derived from human α-synucleinopathy brains (21). Such filaments were never detected in the Sarkosyl-insoluble fraction of cells solely overexpressing α-syn (data not shown). These results indicated that the biochemical characteristics of α-syn accumulated in cells forming the Lewy body-like inclusions

FIGURE 2. **Confocal laser and electron microscopic analyses of α-syn inclusions in plasmid-derived α-syn-expressing cells treated with seed α-syn.** *A–D*, confocal laser microscopic analyses of control SH-SY5Y cells transfected with pcDNA3 vector and Lipofectamine alone (*A*), cells transfected with pcDNA3-α-syn (*WT*) (*B*), cells transduced with the seed α-syn (*Seed αS*) (*C*), and cells transfected with both pcDNA3-α-syn and Seed αS (*WT + Seed αS*) (*D*), immunostained with anti-Ser(P)^{129} (*green*), and counterstained with TO-PRO-3 (*blue*). The *arrows* indicate cytoplasmic round inclusions stained with anti-Ser(P)^{129} (*PSer129*). *Scale bars*, 20 μm. *E–F*, comparison of confocal images of cells transfected with both α-syn plasmid and Seed αS (*E*) and tissue sections from DLB brains (*F*) using anti-Ser(P)^{129} (*green*) and anti-ubiquitin antibodies (*red*). Cytoplasmic inclusions in transfected cells (*arrows*) are positive for ubiquitin, like Lewy bodies (*arrowheads*) in DLB brains. *Scale bars*, 20 μm. *G* and *H*, confocal microscopic images of cells transfected with both pcDNA3-α-syn and Seed αS. Cells were stained with 0.05% Thioflavin S (*green*) and anti-Ser(P)^{129} antibody (*red*). The *boxed area* on the *left* is shown in the *right panel*. *Scale bars*, 20 μm on the *left* and 10 μm on the *right*. *I* and *J*, electron microscopic analyses of cells transfected with both pcDNA3-α-syn and Seed αS. High magnification of the boxed area in *I* is shown in *J*. An *asterisk* or *arrow* indicates a nucleus or mitochondrion, respectively. *Scale bars*, 2 μm in *I* and 200 nm in *J*. *K*, immunoelectron microscopic observation of cells transfected with both pcDNA3-α-syn and Seed αS using a polyclonal antibody against phosphorylated Ser^{129} of α-syn. *Scale bar*, 200 nm.

were very similar to those of α-syn deposited in the brains of patients with α-synucleinopathies, including PD and DLB.

Because the idea has been gaining ground that transient oligomers, rather than mature fibrils, are responsible for cytotoxicity, we examined whether soluble oligomers could be introduced into cells in the same manner as fibril seeds by means of LA treatment and whether they could function as seeds for intracellular α-syn aggregate formation. As shown in Fig. 4, *A* and *B*, we purified stable α-syn oligomers from recombinant α-syn treated with exifone, an inhibitor of *in vitro* α-syn aggregation, which is thought to inhibit filament formation of α-syn by stabilizing SDS-resistant soluble oligomers (22, 23). Then cells expressing α-syn or mock plasmid were treated with a mixture of the oligomer fraction (5 μg) and LA and incubated for 3 days. Immunoblot analyses of lysates of these cells did not detect any SDS-resistant soluble oligomeric α-syn, and the levels of phosphorylated α-syn in the Sarkosyl-soluble and -insoluble fractions showed no increase (Fig. 4, *C* and *D*). On the other hand, we observed phosphorylated and deposited α-syn in the Sarkosyl-soluble and -insoluble fractions in cells expressing α-syn treated with Seed αS (Fig. 4, *C* and *D*). These results showed that SDS-resistant soluble oligomer of α-syn could not be introduced into cultured cells in the same manner as monomeric α-syn and/or could not function as seeds for intracellular α-syn aggregation.

Mutagenic Analysis of Nucleation-dependent Assembly of α-Syn—To investigate further the nucleation-dependent polymerization of α-syn, we analyzed the polymerization of α-syn mutated or truncated at various residues or subdomains that are believed to be crucial for its aggregation. Overexpression of A53T familial Parkinson mutant α-syn, which is readily fibrillogenic *in vitro*, in the presence of Seed αS moderately increased the accumulation and phosphorylation of α-syn in the Sarkosyl-soluble and insolu-

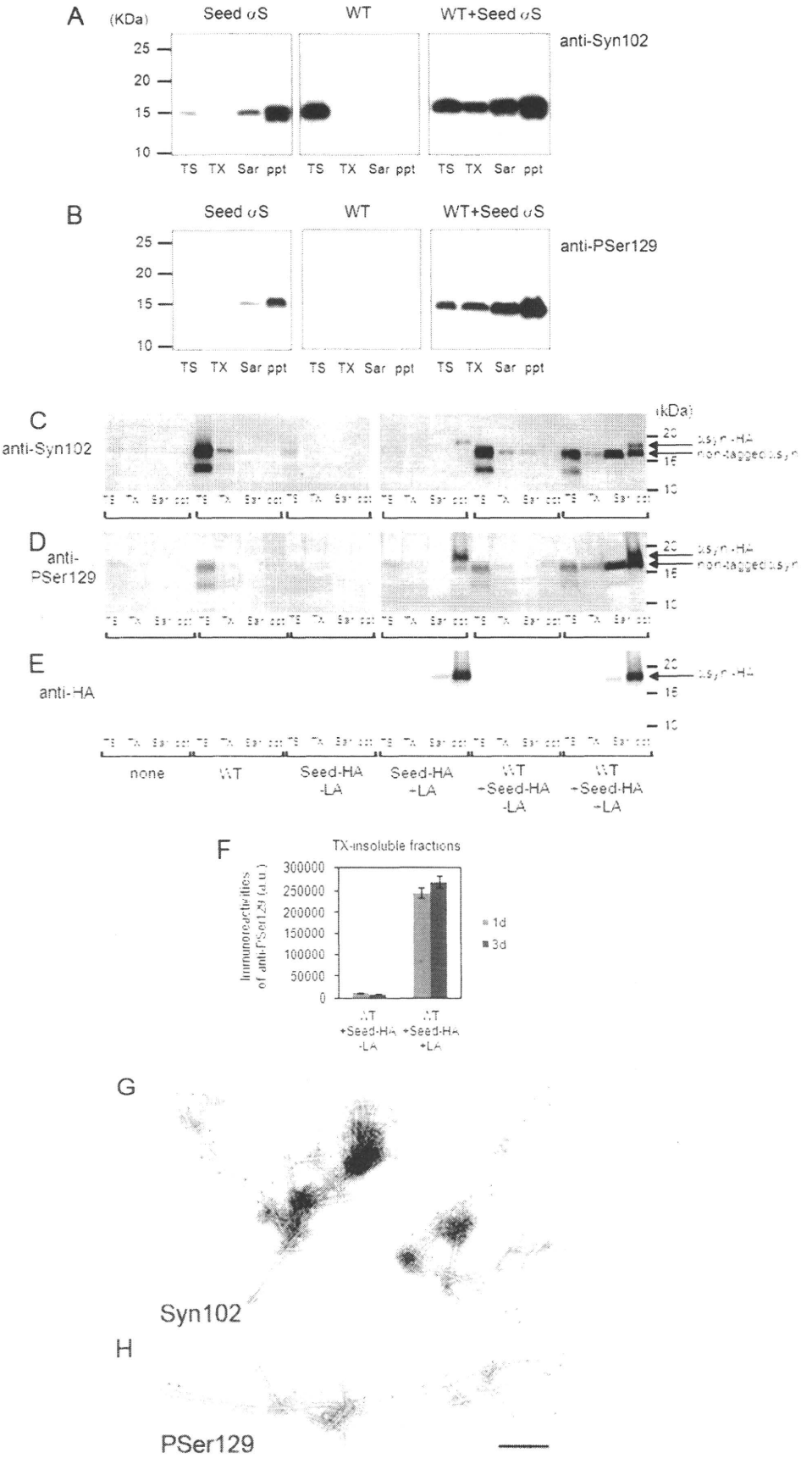

ble fractions compared with those in cells with wild-type α-syn expression and Seed αS (Fig. 5, *A* and *B*). In contrast, overexpression of Δ11 mutant α-syn, an assembly-incompetent mutant lacking residues 73–83, which have been shown to be essential for fibril formation of α-syn (24), elicited neither deposition nor phosphorylation of α-syn. We next introduced α-syn into SH-SY5Y cells expressing S129A mutant α-syn and observed slightly lower levels of Sarkosyl-insoluble α-syn compared with those in cells with wild-type α-syn expression and Seed αS. However, the frequency of inclusion bodies observed in seed-transduced cells expressing S129A was similar to that in seed-transfected cells expressing wild-type α-syn (data not shown), suggesting that phosphorylation at Ser^{129} is not required for the nucleation-dependent polymerization of α-syn within cells.

Nucleation-dependent Intracellular Polymerization of α-Syn Elicits Neurotoxicity and Cell Death—SH-SY5Y cells overexpressing α-syn started to show marked clumping suggestive of cellular degeneration and death by ~48 h after introduction of seeds (Fig. 6*B*). Quantitative analysis of cell death by a lactate dehydrogenase (LDH) release assay at 72 h after introduction of Seed αS showed that cells overexpressing wild-type, A30P, A53T, or S129A α-syn released ~30% of total LDH from total cell lysate, whereas only ~12% of LDH was released from cells expressing Δ11 mutant α-syn, which lacks polymerization ability. In control cells transfected with empty vector or pcDNA3-α-syn followed by treatment with Lipofectamine without seeds, only ~7% of LDH was released (Fig. 6*C*). These results suggest a close correlation between the seed-dependent aggregation of α-syn and cell death. However, the dying cells transfected with fibrillization-competent α-syn and seeds did not show typical morphological changes of apoptosis (*e.g.* nuclear fragmentation, positive TUNEL staining (supplemental Fig. S4*A*), or activation of caspase-3 (supplemental Fig. S4*B*)), suggesting that they did not undergo typical apoptotic cell death, despite a previous report that exposure to neuron-derived extracellular α-syn may cause apoptosis (25).

Impairment of Proteasome Activity in Cells with Intracellular Aggregates of α-Syn—Because α-syn is ubiquitinated in the brains of patients with α-synucleinopathies (26) and inhibition of ubiquitin-proteasome systems by aggregates of proteins with expanded polyglutamine tracts has been reported (27), we analyzed the ubiquitination state of cellular proteins in α-syn aggregate-forming cells and compared the pattern with that in cells treated with a proteasome inhibitor, MG132. A Sarkosyl-soluble fraction of seed-transduced cells expressing wild-type α-syn and harboring abundant inclusions showed increased levels of ubiquitin-positive staining, which was similar in pattern to that observed in cells treated with MG132 (Fig. 6*D*). Because this pattern suggested an impairment of the ubiquitin-proteasome system, we directly analyzed the proteasome activity of α-syn inclusion-forming cells using a specific fluorescent peptide substrate, benzyloxycarbonyl-Leu-Leu-Glu-7-amido-4-methylcoumarin, that emits fluorescence following proteasomal digestion and confirmed that proteasome activity was significantly reduced in these cells as well as in cells treated with 20 μM MG132 for 4 h (Fig. 6*E*). We further examined the suppression of proteasome activity using CL1, a short degron that has been reported to be an effective proteasome degradation signal (28) and whose fusion protein with green fluorescent protein (GFP-CL1) has been used as a reporter for inhibition of proteasomal activity by intracellular polyglutamine aggregates (27) and intracellular α-syn (19). To examine if intracellular α-syn inclusions affected proteasomal activity, SH-SY5Y cells were transfected with both wild-type α-syn and GFP-CL1, followed by the introduction of Seed αS. Fluorescent signals of GFP were scarcely detected in control cells transfected with GFP-CL1 alone (Fig. 6*F*, *none*) but were markedly increased upon treatment with proteasome inhibitor MG132 (Fig. 6*F*, *MG132*), confirming that GFP-CL1 was effectively degraded by proteasome. Strikingly elevated GFP signals were detected in cells forming α-syn inclusions (Fig. 6*F*, *WT + Seed αS*) compared with those in control cells (Fig. 6*F*, *none* or *WT*), and GFP-CL1 and deposits of phosphorylated α-syn were co-localized within these cells (*arrowheads*). These results strongly suggest that proteasome activity is impaired in cells harboring α-syn inclusions elicited by the introduction of Seed αS.

Small Molecular Inhibitors of Amyloid Filament Formation Protect against Cell Death Induced by Seed-dependent α-Syn Polymerization—We have previously shown that several classes of small molecular compounds inhibit amyloid filament formation of α-syn, Tau, and Aβ *in vitro* (17, 23). These observations prompted us to test whether these inhibitors exert a protective effect against death of SH-SY5Y cells mediated by the nucleation-dependent polymerization of α-syn. Fig. 7*A* shows the effects of three polyphenol compounds, exifone, gossypetin, and quercetin, and a rifamycin compound, rifampicin, added to the culture media at a final concentration of 20 or 60 μM. Remarkably, all of these compounds blocked cell death, with gossypetin being the most effective. Our previous *in vitro* studies elucidated that several polyphenols, including gossypetin and exifone, inhibit α-syn assembly and that SDS-stable, noncytotoxic soluble α-syn oligomers are formed in their presence (23), suggesting that such polyphenols may inhibit filament formation of α-syn by stabilizing soluble, prefibrillar intermediates. Gossypetin or exifone might suppress intracellular α-syn aggregate formation by stabilizing such soluble intermediates in cultured cells as well. Immunoblot analysis

FIGURE 3. **Immunoblot and immunoelectron microscopic analyses of intracellular α-syn aggregates in cultured cells.** *A* and *B*, immunoblot analysis of α-syn in cells treated with Seed αS alone (*Seed αS*), pcDNA3-α-syn alone (*WT*), or both WT and Seed αS (*WT + Seed αS*). Proteins were differentially extracted from the cells with Tris-HCl (*TS*), Triton X-100 (*TX*), and Sarkosyl (*Sar*), leaving the pellet (*ppt*). Blots were probed using anti-α-syn (Syn102) (*A*) and anti-$Ser(P)^{129}$ (*PSer129*) (*B*). *C–F*, immunoblot analysis of proteins differentially extracted from mock (none) or cells transfected with pcDNA3-α-syn (*WT*), cells transduced with Seed-HA with (*Seed-HA + LA*) or without LA treatment (*Seed-HA − LA*), and cells overexpressing α-syn treated with Seed-HA with (*WT + Seed-HA + LA*) or without LA treatment (*WT + Seed-HA − LA*). Immunoreactivity of phosphorylated α-syn in the Triton X-100-insoluble fraction was quantified using anti-$Ser(P)^{129}$, and the results are expressed as means ± S.E. ($n = 3$), as shown in *F*. a.u., arbitrary unit. *G* and *H*, immunoelectron microscopy of α-syn filaments extracted from transfected cells. SH-SY5Y cells were transfected with both pcDNA3-α-syn and Seed αS. Sarkosyl-insoluble fraction was prepared from the cells, and the filaments were immunolabeled with anti-Syn102 (*G*) or $Ser(P)^{129}$ (*H*) antibody. *Scale bar*, 200 nm. *1d* and *3d*, 1 and 3 days, respectively.